Personnel Airdrop Risk Assessment Using Bootstrap Sampling

THESIS

Wonsik Kim
Major, Republic of Korea Army

AFIT/GOR/ENS/96D-01

DEPARTMENT OF THE AIR FORCE
AIR UNIVERSITY
AIR FORCE INSTITUTE OF TECHNOLOGY

Wright-Patterson Air Force Base, Ohio

AFIT/GOR/ENS/96D-01

Personnel Airdrop Risk Assessment Using Bootstrap Sampling

THESIS

Wonsik Kim
Major, Republic of Korea Army

AFIT/GOR/ENS/96D-01

THESIS APPROVAL

STUDENT: Won Sik Kim, Major, ROKA CLASS: GOR-96D

THESIS TITLE: Personnel Airdrop Risk Assessment Using Bootstrap Sampling

DEFENSE DATE: 10 October 1996

COMMITTEE	NAME/TITLE/DEPARTMENT	SIGNATURE
Advisor	T. Glenn Bailey, Lieutenant Colonel, USAF Assistant Professor of Operations Research Department of Operational Sciences Air Force Institute of Technology	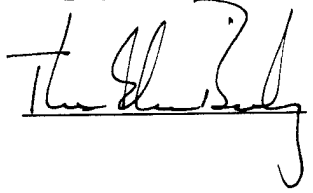
Reader	Dennis C. Dietz, Lieutenant Colonel, USAF Assistant Professor of Operations Research Department of Operational Sciences Air Force Institute of Technology	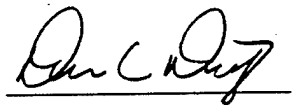

The views expressed in this thesis are those of the author and do not reflect the official policy or position of the Department of Defense or the U. S. Government.

AFIT/GOR/ENS/96D-01

Personnel Airdrop Risk Assessment Using Bootstrap Sampling

THESIS

Presented to the Faculty of the School of Engineering
of the Air Force Institute of Technology
Air University
In Partial Fulfillment of the
Requirements for the Degree of
Master of Science (Operations Research)

Wonsik Kim, B.S.
Major, Republic of Korea Army

December, 1996

Preface

The purpose this study, sponsored by C-17 SPO, was to find a way of minimizing the risk of entanglement using the Bootstrap Method. It is a part of their continuing investigation into the safety problem of paratrooper operations for new aircraft.

I wish to acknowledge those people that have provided guidance and assistance in preparing this thesis. First, a word of thanks to my advisor, Lt Col Glenn Bailey and to my committee member, Lt Col Dennis C. Dietz, for their help and guidance throughout this research. Second, I would like to thank those people at the C-17 SPO who provided advice and data - Col (sel) Randall Davis, Mr. Mark A. Kuntavanish, Mr. Carl B. Mihlbachler and Maj Nancy R. Vetere. Third, I would like to thank my close friends, Lt Col Yunhyok Chang, LCDR Paul Son, Dr. Rainier Lee, Capt Kiho Kang, Capt Yunjin Chong, and Capt Taeho Yun who shared good time with me and led to the success of my research. I am also deeply indebted to Capt Heongyu Park and Capt Hyunki Cho who spent considerable time helping me to speak the language of Fortran and Latex, respectively.

Next, I want to thank my parents and parents-in-law who were praying for me and my family during the completion of this research. I would also like to thank my country for allowing me to have good experience in AFIT.

Finally, most important, I would like to express my deepest gratitude to my children; Yusuk and Yejin; and to my lovely wife, Inhyang, for allowing to play absentee father and husband for the years it took finish this task. My wife's insight and selfless efforts were vital elements throughout this endeavor. She was always there when I needed her help. Thank you.

Wonsik Kim

Table of Contents

List of Figures

List of Tables

List of Abbreviations and Symbols

Abbreviations	*Description*
SPO	system program office
CINE-T	cinetography Theodolite
DOE	design of experiments
CFD	computational fluid dynamics
CLT	central limit theorem
MLE	maximum likelihood estimate
KTM	kineto track mount
ASP	airborne space positioning
PAO	personnel airdrop optimization

Abstract

Previous work on personnel airdrop problems involving jumpers has been event-oriented – entanglement rates, number of canopy "bumps", landing injuries, and deaths represent the typical metrics. The thesis expands this area of research by developing cumulative distribution functions of maximum possible chute entanglement risk for the C-17 using bootstrap techniques. By comparing the effects of various C-17 aircraft configurations on the entanglement CDF, this thesis shows that under certain configurations the risk of centerline entanglement for the C-17 is less than that for the C-141.

Personnel Airdrop Risk Assessment Using Bootstrap Sampling

I. Introduction

1.1 Background

In the military, personnel airdrop is a method the army and other special forces use to deploy ground forces inside enemy territory covertly and swiftly. The personnel involved are transported via carrier aircraft in day or night to parachute down to the designated target area. During the airdrop the personnel line up in two columns – equipped with parachute, weapons and other survival gear – and exit from the aircraft's left and right side.

In order for these airdrop operations to go smoothly, the military must constantly train its members. These exercises present several safety problems such as parachute entanglement, deployment bag strikes, parachutes not deploying, and personnel injury during landing. Parachute entanglement occurs when the parachute or equipment of a jumper becomes entangled with another jumper's parachute during the airdrop, or when the parachute canopy contacts some part of the aircraft. D-bag strikes occur when the deployment bags of previous jumpers strike the next jumper. Parachute non-deployment occurs when the parachute fails to open due to faulty packing. Finally, personnel injury during landing occurs for many reasons, such as lack of training, catching trees, falling in ground pot holes, hitting some foreign object such as a rock, or injury by their own equipment as they land. Several of these problems are controllable, such as the parachute not deploying, entanglement, and D-bag strikes. Others are uncontrollable, such as personnel injury during landing, weather, wind speed, etc.

Historically, safety issues related to the military airdrop operations have involved event-oriented response data. Typical data include reportable injuries or deaths per 10,000 jumpers, the number of high-altitude or low-altitude jumper entanglements per 10,000 jumpers, and the number of observed canopy contacts (per 100 jumpers) between the jumper and some portion of the aircraft [1]. Thus, one can view paratrooper operations as a random process where the random variable of interest, say the number of entanglements that occur in n jumpers, would have a *discrete* distribution (e.g. Binomial with some probability of "success" p, where the parameter p would be estimated using the above empirical rates). This type of analysis is satisfactory for determining the risk for existing systems, since empirical data is available for estimating the parameters. However for new systems (specifically the C-17), it is necessary to develop *continuous* response variables in order to minimize the risk of entanglement. Lawson's (1995) approach discusses the development of these responses, the experimental design used to explore configuration changes that would reduce the risk to paratroopers jumping from the C-17 aircraft, and the estimated distribution function of the new response variable (jumper-to-jumper separation) for the altered configuration (12). This thesis analyzes the reduction of the risk of entanglement for the C-17 as compared to the C-141. The remainder of this section will give additional background for this problem.

1.2 Research Objective

The C-17 System Program Office (SPO) and US Army are interested in airdrop problems, such as entanglement, canopy contacts and D-bag strikes. Specifically, these organizations are interested in (i) the D-bag strike potential of the C-17, and (ii) characterizing the centerlining tendency of C-17 as compared with C-141. They wish to know which factors (variables) affect these responses, the magnitude of these

[1] US Army Safety Center Data for the period of 1980 - 1989 indicates 0.01%(1 in 10,000 jumpers) entanglement injury rate for C-141 jumps.

effects, and whether the risk of entanglement and D-bag strikes of the C-17 is lower than the C-141.

This thesis is primarily concerned with the probability of jumper-to-jumper entanglement when paratroopers jump from an aircraft. The binary response variable, jumper-to-jumper entanglement, gives the U.S. Army and the U.S. Air Force the most direct indication of the risk of deleterious events associated with paratrooper operations for current systems. However, this type of data is not always well-suited for process improvement or parameter design. Aside from definitional problems and potential under-reporting of these binary responses, the likelihood of these events is (fortunately) quite low. Therefore, studying process improvement issues with a binary response variable requires enough test observations to generate a reasonable number of occurrences.

The objective of this research is to verify that the risk of entanglement from the C-17 is lower than C-141 using a bootstrap confidence interval. This study contains three sub-objectives, which provide a solution to the research problem. These sub-objectives are:

- Investigate the sources and characteristics of the representative data;
- Explore methodologies for addressing the problem; and,
- Identify/recommend a technique that solves the problem.

This study is limited in scope by the data provided by the C-17 SPO. The data generated by the C-17 SPO and U.S. Army while testing the effect of gross weight and static line length on separation of C-17 dual-door jumpers, and the separation of jumpers from the D-bag cluster, will be the basis for the thesis. However, there are several problems encountered during the required testing and analysis.

First, due to time and rising flight test costs, the average quantity of data is limited. Second, since calculating the free fall body in an exact manner is not feasible, there will be some process variabilities in the obtained data. Third, static line length,

jumper exit style, aircraft weight and aircraft equipment factors all influence the outcome. Fourth, jumper exit style influences the jumper's trajectory, speed, and direction. Fifth, aircraft speed and pitch can affect the test results. Finally, as mentioned in Section 1.1, uncontrollable factors of airdrops such as weather, wind speed and personnel injury during landing are not considered.

1.3 Overview

This chapter provides a background to understanding the risk of entanglement and the D-bag problem in paratroop jumps from the aircraft; presents the thesis objective; and, identifies the scope and limitations of the study. The next chapter discusses the relevant literature, while Chapter III describes in detail the methodology used to achieve the research objectives. Chapter IV presents the findings and analytical results. Finally, Chapter V discusses the significance of the findings, draws conclusions, and suggests areas for further research.

II. Review of the Literature

2.1 Introduction

The purpose of this review is to discuss the literature relevant to this research. This chapter will discuss the data sources of the study, and methods for analyzing the data. In Section 2.2, we discuss Lawson's (1995) experimental design used to find best configuration and significant variables.

2.2 C-17 Experimental Results

Lawson (1995) employs an experimental design described below to select a configuration for the C-17 that improves paratrooper safety (12). His response variables are both closely related to entanglement incidents and useful for detecting differences between alternative configurations; thus this research has a close relationship to Lawson's. Therefore, this section is a synopsis of his experimental results.

Experiments are performed by investigators in many fields of inquiry to discover something about a particular process or system. The objectives of the experiment include the following:

- Determining which variables are most influential on the response.
- Deciding where to set the influential variables so that the response variable is almost always near the desired nominal value.
- Considering where to set the influential variables so that variability in the response variable is small.
- Resolving where to set the influential variables so that the effects of the uncontrollable variables are minimized (14).

2.2.1 Definitions. Usually we define a *response* as a variable of interest which can be influenced by experimental conditions, and *factors* as those variables

which can affect one of several possible responses. Also we define *levels* as the value at which a given factor will be set – in this case two levels for most of the factors. A test matrix provides the factor-level combinations at which a response will be measured. Lawson assumes that all factors in the test matrix are *controllable factors* during normal operations. He defines a *run* as the portion of the test done to generate a single response variable value for a specified set of factor-level combinations. Also he defines a *centerline* as a imaginary line which equally splits the aircraft in a lengthwise direction. A *replicate* is defined as a repeat of the basic experiment. The goal of his experiment is to determine the factor-level combinations which yield the most desirable and least varying response values (12).

2.2.2 Coordinate System. A trajectory is characterized by the 4-tuple (X, Y, Z, t). The distance traveled (in feet) is represented by X; the distance from the centerline is Y; the vertical distance is Z; and time (in seconds) is t. Positive X is off the nose of the aircraft (jumpers travel in the positive X direction). Positive Y is off the left-wing, while positive Z is upward. The origin $X = 0$ is at the position of the left or right door when the person jumps; $Y = 0$ on the aircraft centerline when the person jumps; $Z = 0$ at the height of the floor when the person jumps; and, $t = 0$ at the moment when the person steps or jumps off the exit ramp (12).

2.2.3 Configurations. Digitized data was taken in November 1994 from a C-17 using a system for taking trajectory data constrained to one jumper per "pass". The aircraft flew at 135 knots with a 2° deck angle with the initial response variable the distance between the centerline of the aircraft and the apex of the chute when the chute first becomes fully open. Figure 2.1 shows the histogram and estimated density for this metric based on a sample of 20 jumpers from each door. Subsequent analysis using these distributions – along with the distribution of the exit time difference for opposite-side, nearest neighbor pairs – estimated a probability that a random jumper was separated from his closest neighbor by d feet at the time of full

open. This probability can be written as

$$P(S_{C-17} \leq d) \tag{2.1}$$

where S_{C-17} is a random variable denoting separation (in feet) between jumpers in a nearest-neighbor pair at the full-open point for the C-17, and d is a constant (S_{C-141} designates the equivalent random variable for the C-141). Estimated probabilities for selected values of d are shown in Table 2.1.

distance d	$d = 24.5$	$d = 18{,}375$	$d = 12.25$	$d = 6.125$
$P(S_{C-17} \leq d)$	.09665199	.06788232	.04337461	.01858151

Table 2.1 Estimated Probability (Jumper Separation at full open $\leq d$) prior to changing the paratrooper drop configuration for the C-17 (12).

The fact that roughly 10% of jumpers were estimated to be within 24.5 feet (the diameter of T-10 parachute) was not out of line with Lawson's expectations. However, it was desirable for $P(S_{C-17} \leq d) < P(S_{C-141} \leq d)$ for $0 < d < \infty$: i.e., for a given distance d the C-17 would provide a smaller probability of encounter from the C-141 (12).

2.2.4 Responses. The primary response for the experiment was the minimum distance between two trajectories in a given run. The digital records (time, x, y, and z) of one left and one right trajectory (taken in separate passes of the aircraft) were required to compute one value of this variable. A secondary response was the area between the door-line and one trajectory on the same side. The Cinetography Theodolite (CINE-T)[1] system was used to obtain baseline data for the C-141 as well as the baseline and the reconfigured C-17. This system was limited to one jumper per pass, but tracked both the body and the chute apex, thus allowing a computed "center".

[1]CINE-T is a measurement system consisting of a set of multiple 35 mm movie cameras tracking an object for XYZ-axis positions.

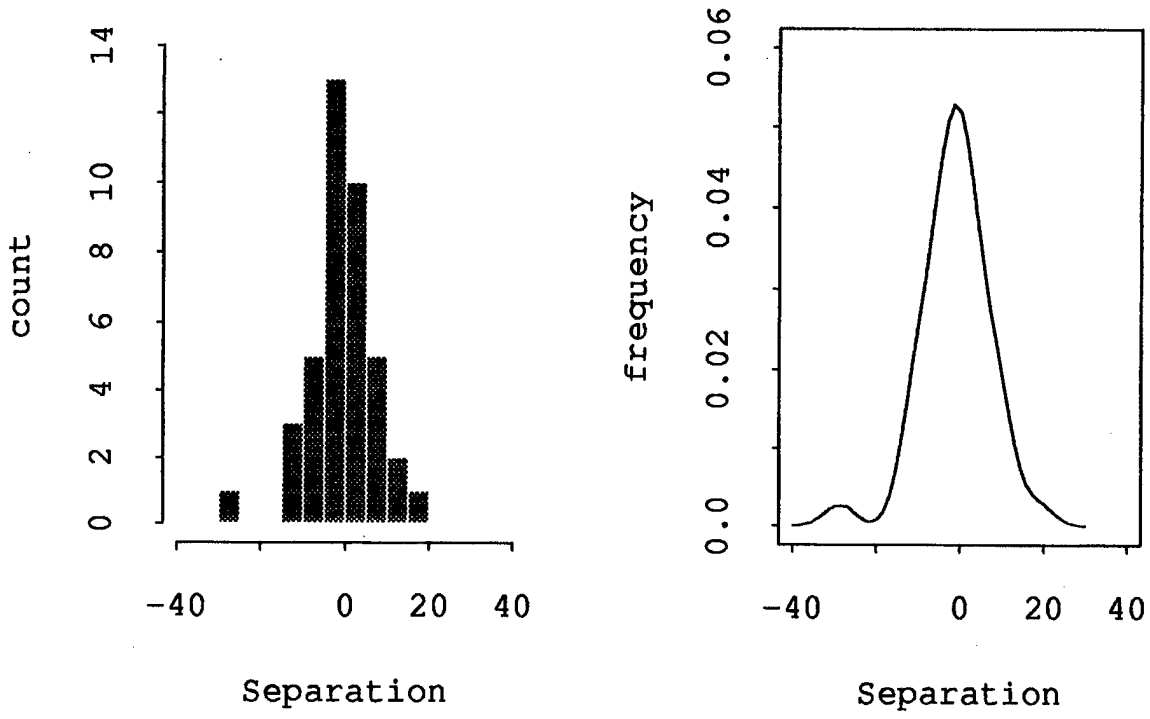

Figure 2.1 Histogram and Density for the C-17 distance between Aircraft Centerline and apex of the chute at full open prior to changing the paratrooper drop configuration (12).

2.2.5 Variables and Metrics. Finding the appropriate variables and metrics of paratrooper trajectories for the Design of Experiments (DOE) is a process unto itself (12). Since some understanding of the phenomena must be used to determine the appropriate variables for the DOE, a multi-disciplinary group determined the variables using known physics, deterministic computer models, and individual experience. This section describes their recommendations (12).

A large group of potential variables (referred to as *factors*) were culled by the group into those that were considered to be the most important. These included aircraft speed, flap setting, landing gear configuration, jumper weight, static line length, and jumper exit style. (Later Lawson found that aircraft weight would also

be important (12).) The first five factors were tested at two *levels* each, while three types of exit style were tested.

The group also decided to run a second experiment to consider break-tie (connects deployment bag to parachute pack) strength, parachute ring slider, position of the anchor point, and a modified deflector door. Assessing the effect of these factors at various aircraft settings required including the factors of speed, flaps, and landing gear. Since these factors were not safety-released for live jumpers, this experiment was conducted using mannequins.

The DOE required the use of a singleton response for each set of factor settings tested. This response is needed to describe the most relevant features of the dynamic phenomenon, and has to be calculated from the digitized paratrooper trajectory data (provided in the form of position vectors in time). This digital data was obtained using six camera theodolites which together produced output used to triangulate the position of a tracked object.

The metrics used as the response variables were the minimum approach distance between a left and right jumper's trajectory, and a variable that recorded the total tendency of the trajectory to go towards the centerline of the aircraft. The minimum approach distance was used by the DOE as the primary response variable. The centerlining tendency variable was used to ensure consistent results for the live-jump experiment and was the primary response variable for the mannequin experiment.

A computer algorithm was written to compare the digitized trajectories and to compute the centerlining tendency response for each trajectory. The minimum distances were computed from comparison between one left and one right trajectory. The comparison included a range of time delays for both of the trajectories in a "matchable" pair (to be matchable, the two trajectories had to be from opposite sides and flown under the same speed, flap, and gear settings). The centerlining tendency response was the area projected by the trajectory onto the $X - Y$ plane

inside the door line. If the trajectory did not pass inside the door line then the value was zero. If the trajectory did pass inside the door line , the amount it had traveled was multiplied by the corresponding down range travel and added to any previous values of the centerlining response (see Figure 2.2). The advantage of this response

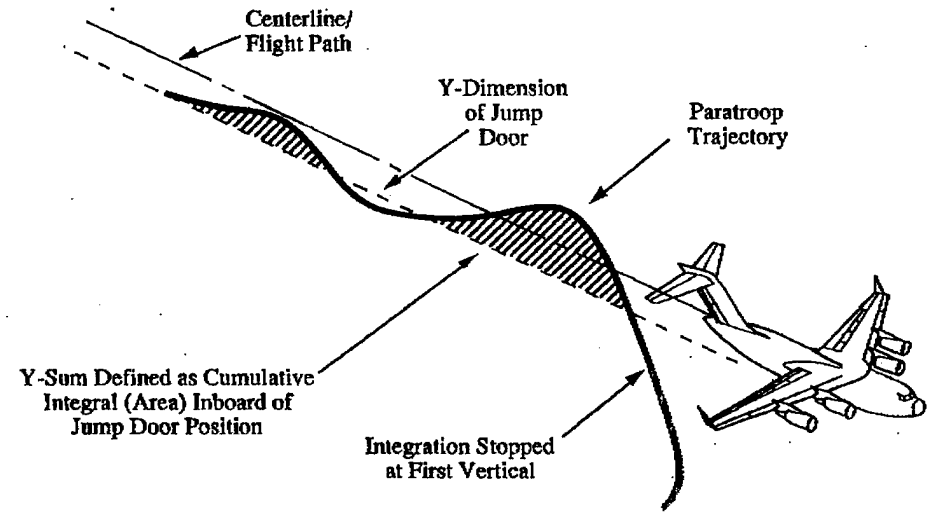

Figure 2.2 Y-sum Measure of Merit (13).

was that no comparison (with another trajectory) was needed to assess the merit of a given trajectory.

2.2.6 Experimental Design. Experiments involving the study of effects of two or more factors on some response variable of interest can be handled very efficiently by a *factorial design.* For a full factorial design, one replication consists investigating all possible combinations of the levels of each factor. For example, one replication of a full factorial design involving 6 factors, each at 2 levels, would involve $2^6 = 64$ runs. Factorial experiments can provide the advantage of providing estimates of the effects (of the factors) on the response variable that are just as precise as one factor-at-a-time experiments, while requiring substantially fewer runs (14). (For this example of 6 factors, each at 2 levels, the relative efficiency of the factorial design to

the one-factor-at-a-time experiment is approximately 3.5.) A further savings in the number of runs can be attained if we can assume that *high-order* interactions are negligible. In this case, information on the main effects (for example, Speed × Gear) may be obtained by running only a fraction of the complete factorial experiment. Lawson used a design which allowed him to estimate all main effects and two-way interaction effects.

A convenient paradigm for his purpose was to treat the variables in Table 2.2 as "controllable factors", along with the levels those factors can assume during the experiment. Table 2.3 lists the levels the uncontrollable (noise) factor can assume. Taking the view advocated by Byrne and Taguchi (4), the DOE was structured to find the levels of the controllable factors that were the least influenced by the noise factors and that provided the largest minimum distance between a left and right trajectory. For this experiment, the exit style was treated as uncontrollable for routine operations, even though it can be controlled for the purposes of the test. This allows the design to estimate the variance associated with the controllable factors.

		Level	
Label	*Factor*	1(-)	2(+)
A	Aircraft Speed	135 knots	125 knots
B	Aircraft Flaps	35°	25°
C	Landing Gear	Up	Down
D	Right Static Line	15′	20′
E	Left Static Line	15′	20′
F	Right Weight	225±	300±
G	Left Weight	225±	300±

Table 2.2 Controllable Factors for the Inner Array (12).

Label	*Description*	1	2	3
H	Exit Style	45°, walk out	90°, kick out	90°, vigorous, feet in

Table 2.3 Uncontrollable Factor for the outer Array (12).

Inner Array								*Outer Array*	
	Variables								*Variables*
Run	*A*	*B*	*C*	*D*	*E*	*F*	*G*	*Run*	*H*
1	1	1	1	1	2	1	2	1	1
2	1	1	1	2	2	2	1	2	2
3	1	1	2	1	1	2	1	3	3
4	1	1	2	2	1	1	2		
5	1	2	1	1	1	2	2		
6	1	2	1	2	1	1	1		
7	1	2	2	1	2	1	1		
8	1	2	2	2	2	2	2		
9	2	1	1	1	1	1	1		
10	2	1	1	2	1	2	2		
11	2	1	2	1	2	2	2		
12	2	1	2	2	2	1	1		
13	2	2	1	1	2	2	1		
14	2	2	1	2	2	1	2		
15	2	2	2	1	1	1	2		
16	2	2	2	2	1	2	1		

Table 2.4 Each run from the inner array requires a left and a right jump, each at 3 exit style (from the outer array), for a total of 96 individual live jumps (12).

The design matrix shown in Table 2.4 consists of an inner array of 16 runs and an outer array of 3 runs. In the Taguchi form (Ross 1988), each of the 16 runs of inner array is tested across the 3 runs of outer array for total of 48 runs. (This experimental design is also equivalent to a $3 \times 2^{7-3}$ fractional factorial (2).) Obtaining a response (minimum distance) for a given run required a left jump and a right jump, for a total of 96 individual live jumps.

Recalling that a trajectory was characterized by the 4-tuple (X, Y, Z, t), Lawson used a random number generator to assign the order of the runs to guard against falsely attributing some effect to a factor which is in fact due to some variable outside of experimental control (12). For example, if the strength of the cross wind increases from 5 knots in the morning to 15 knots in the afternoon, he did not want all of the

reduced flap runs to be in the afternoon, since doing so could either cause or negate an effect.

Label	*Factor*	*Level*	
		1 (-)	2 (+)
A	Landing Gear	Down	Up
B	Break-Tie	160 pounds	320 pounds
C	Aircraft Speed	135 knots	125 knots
D	Aircraft Flaps	35°	25°

Table 2.5 Two-level Factors for the Mannequin Drop Test Matrix. A fifth factor, Air Deflector, was tested at 3 levels. All factors were viewed as "controllable" for test and operational purpose (12).

Because of the number of factors under investigation, and the safety clearances required for some of those factors, a limited experiment using mannequins was conducted. Lawson used the trajectory centerlining variable as the response for this experiment, so that each run could be obtained from a single trajectory. The variables shown in Table 2.5 define the first four factors and levels for the mannequin drop experiment. A fifth factor, the Air Deflector (E), was tested at three levels. A full factorial experiment (3×2^4) was done, involving 48 drops from the right door only. Each run in Table 2.6 was repeated three times, one for each air deflector level. As with the live jump experiment, Lawson used a limited randomization scheme (12).

2.2.7 Physical Problem. Although people have parachuted from air vehicles since before the invention of powered flight, the physics involved is less predictable than that relevant to sending a human into space. The assessment of paratrooper safety for an aircraft remains a process of observing results without a complete understanding of the phenomena. Only the most basic ballistic three degree of freedom models (integration of a system of three force equations) exist to yield some predictive understanding, which is inadequate to provide a fully quantitative result.

Test Matrix				
	Variables			
Run	*A*	*B*	*C*	*D*
1	1	1	1	1
2	1	1	1	2
3	1	1	2	1
4	1	1	2	2
5	1	2	1	1
6	1	2	1	2
7	1	2	2	1
8	1	2	2	2
9	2	1	1	1
10	2	1	1	2
11	2	1	2	1
12	2	1	2	2
13	2	2	1	1
14	2	2	1	2
15	2	2	2	1
16	2	2	2	2

Table 2.6 Mannequin Drop Experiment. Each run from the Test Matrix required a single right door at a constant weight (250 pounds). Each run was repeated 3 times, 1 for each Air Deflector setting. Only the trajectory centerlining response variable was computed for this experiment, since he only observed single trajectories. The actual jump sequence number was randomly set (12).

The dynamics involved in paratrooper trajectories involve many nonlinear or unquantified forces, with the aerodynamics constituting a large source of unpredictability. Classical and new methods for the assessment of the aerodynamic forces involved are wind tunnel testing and computational fluid dynamics (CFD), respectively. Both of these methods involve great expense for the less complex problem of the aerodynamics of "slender" bodied aircraft (aircraft length is large compared to wake width), though even in this case full fidelity is still not completely achieved. Unfortunately, a jumper is a "blunt" body with a rough, irregularly shape and a mostly loose cloth-covered surface. Furthermore, a jumper's shape may change in

response to muscle movement or applied force. Wind tunnel tests for a full scale combat equipped jumper would have to be done for a full range of speeds, and limb configurations. Also, the local flow about the rear of the aircraft would have to be mapped either with the wind tunnel method (the scale of the model would cause some error here) or by using a CFD solution (error depends on the fidelity of the model). Thus, no analytical techniques presently exist for this case, and a full computational solution (including viscosity terms) would involve massive computational power.

The same difficulties mentioned above also apply to the extremely complex aerodynamic characteristics of parachutes. If the above problems could be solved, the information could be integrated into a six degree of freedom computer model (three force and three moment equations). However with the limited data available for the general aerodynamic force coefficients of the human body, a parachute force time curve for the T-10 parachute, and the possible jumper weights, a three degree of freedom computer model was generated instead. While the model could not predict the "centerlining tendency" of jumper trajectories, and the length of the static line had little effect, it was useful in giving insight to the dynamics of the trajectories (12).

2.2.8 Result. An analysis of variance procedure was used to evaluate the results of both the live-jump and the mannequin experiments. The live-jump experiment used both the minimum distance and the trajectory-centerlining variable as the response. While the same main effects were found on both experiments, differences occurred in the confidence level of contained responses. The mannequin experiment could only use the trajectory-centerlining variable, since mannequins were dropped from only one side.

Using the minimum distance response variable, Lawson found main effects for gear (significant at the 90% confidence level), speed (80%), and flaps (80%), with the

Mean		*Signal-to-Noise*	
Significant Factor	*Best level*	*Significant Factor*	*Best level*
Landing Gear	Up	Landing Gear	Up
Exit Style	90° Vig 90° Kick	N/A	N/A
Left Jumper Wt.	225 lb	Left Jumper Wt.	225 lb
Speed (80%)	125 knots	N/A	N/A
Flaps (80%)	25°	N/A	N/A

Table 2.7 Factor-level settings which produce a higher average minimum distance between jumpers (significant at 90%, unless indicated) and a lower signal-to-noise ratio (12).

best levels (in that they produced higher mean minimum distance) being gear up, 125 knots, and 25° flaps, respectively (see Table 2.7). These settings also produced a reduction in variance (across the 3 levels of the noise factor, exit style). Jumper weight for left-side jumpers was also found to be significant (90% confidence) to the 45° exit style. (Note that no variance was estimated for exit style, since this factor was treated as a noise factor.) No other main effects were found from the list of factors in Table 2.2. Figure 2.3 indicates that speed, flap, and gear settings of 125 knots, 25°, and gear up, respectively, provide the most robust configuration with respect to exit style.

Mean		*Signal-to-Noise*	
Significant Factor	*Best level*	*Significant Factor*	*Best level*
Speed	125 knots	Speed	125 knots
Flaps	25°	Flaps	25°
Exit Style	90° Vig 90° Kick	N/A	N/A
Exit Side(80%)	Right	Exit Side	Right

Table 2.8 Factor-level settings which produce a lower average trajectory centerlining values (significant at 90%, unless indicated) for paratroopers exiting from one side (12).

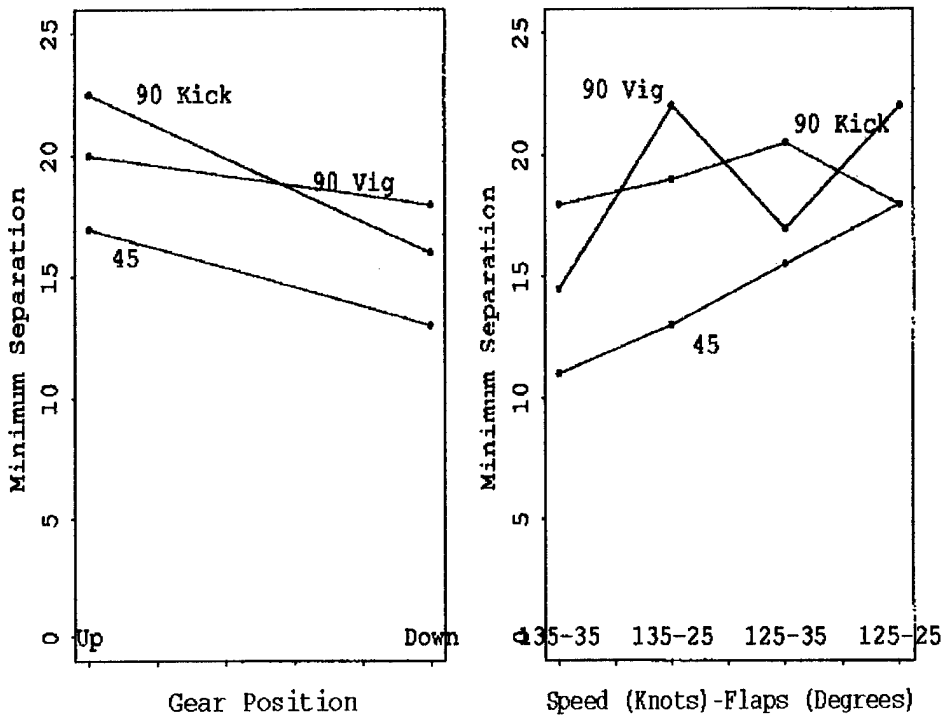

Figure 2.3 *Exit Style vs. Gear Position* and *Exit Style vs. Speed-Flaps* : Factors showing a significant effect on the minimum distance (12).

Table 2.8 gives the results of the analysis of variance using the (single-sided) trajectory centerlining response variable. Since the two response variables were dependent, it is not surprising that the results are similar to those shown in Table 2.7. Speed and flaps are still significant (now at 90% confidence), but here the signal-to-noise ratio is also important. Exit style continues to explain a lot of the variability in the mean response. Gear and left jumper weight are not significant (at 80% or more) when centerlining response variable is used, but exit side is. Figure 2.4 also indicates that speed, flap, and gear setting of 125 knots, 25°, and gear up, respectively, provide the most robust configuration with respect to exit style. Also note that the "90° kick" style was relatively robust to configuration changes, at least within the aircraft gross weight range used for this experiment (330,000 pounds to 360,000 pounds).

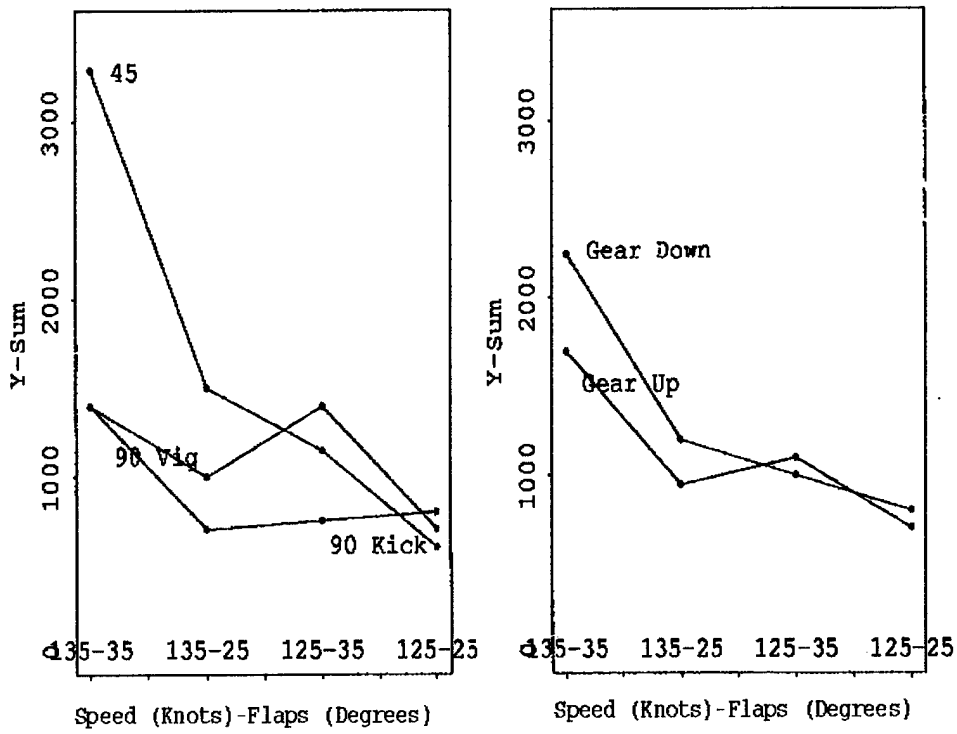

Figure 2.4 *Exit Style vs. Speed-Flaps and Gear Position vs. Speed-Flaps* : Factors showing a significant effect on trajectory centerlining (Y-Sum). Small Y-Sum values are more desirable than large values (12).

The laws of aerodynamics dictate that aircraft speed, flaps, deck angle (pitch), and gross weight are interrelated and co-dependent variables. For example, for a given speed and deck angle, a gross weight setting of 360,000 pounds requires a higher flap setting than a gross weight setting of 330,000 pounds. The desirable speed-flap setting happens to correspond to 7° deck angles, which was the maximum angle approved for personnel airdrop operations. The gross weight range was controlled to be within 330,000 pounds to 360,000 pounds, since the aircraft gross weight changes by approximately 30,000 pounds from start to end of a typical mass jump due primarily to fuel consumption. Higher gross weight settings tend to do worse with respect to the trajectory centerlining variable, since gross weights require more lift and thus higher flap settings.

Mean	
Significant Factor	*Best level*
Break-Tie	160 lb
Speed (80%)	125 knots
Speed × Break-Tie (80%)	160 lb or 135 knots
Speed × Deflector-Type (80%)	Normal Deflector at 135 knots

Table 2.9 Factor-level settings which produce a lower average trajectory centerlining values (significant at 90%, unless indicated) for mannequins exiting from the right side (12). (Note that no signal-to-noise analysis was possible since no duplicate cases were tested.)

Table 2.9 summarizes the results from the mannequin experiment. The standard (160 pounds) apex break-tie is better than the alternative (320 pounds) break-tie, primarily due to better performance at higher speed. There is no significant difference at the lower speed. Overall, the lower speed is better than the higher speed for both live jump and mannequins. The alternate deflector types do not show any improvement over the standard deflector door; in fact, at the higher speed, the standard deflector door does better.

In summary, Lawson found that lower speeds, reduced flaps, and landing gear up produce better trajectories with respect to minimum distance and the trajectory centerlining metric (12). A deck angle of 7° is an equivalent way to specify the reduced flap setting. Since weight made some difference over the specified range, it should stay below 360,000 pounds. The deflector door modifications should not be used, since the best setting is the normal door set at 60°. The break-tie should be kept at 160 pounds of pressure. Based on these recommendations, data was collected on 40 jumpers (20 from each side) with the aircraft flying at 130 knots, landing gear up, and standard break-ties. The aircraft gross weight ranged from 330,000 pounds to 360,000 pounds. Figure 2.5 compares the favorable result of this configuration to that of the November 1994 configuration (Section 2.2.3).

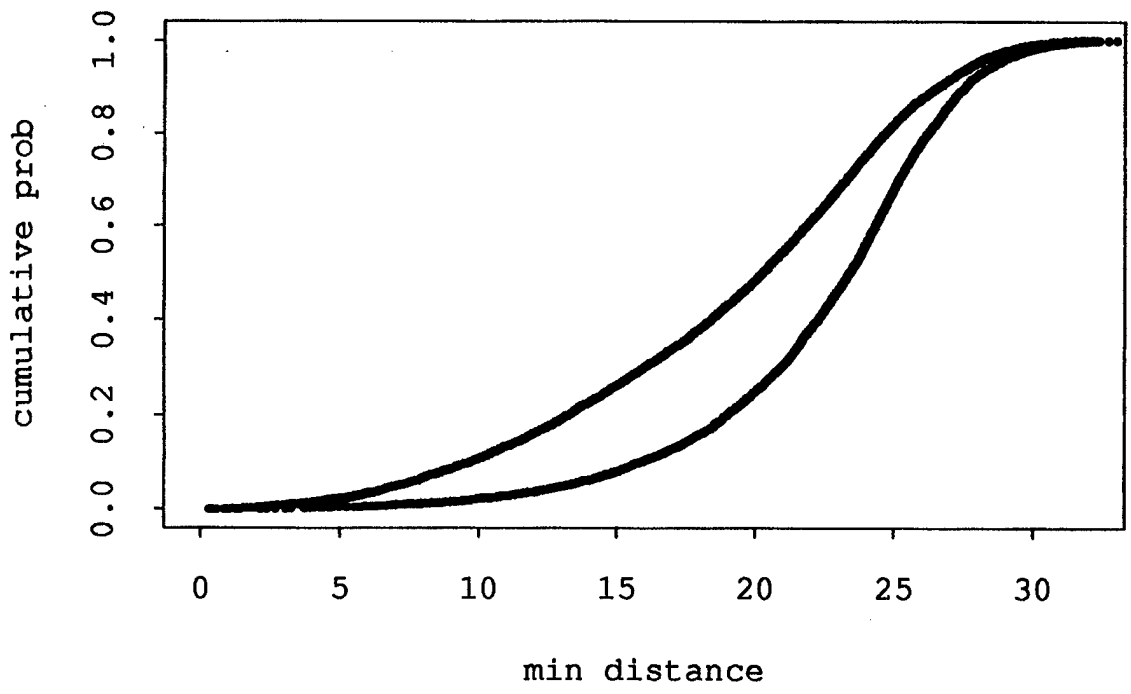

Figure 2.5 Estimated cumulative distribution function for old and new configuration. This chart can be read as the proportion of jumpers expected to be separated by a distance d, where the distance is read from the horizontal axis. The curve for the new configuration is below and to the right of that for the baseline configuration (12).

2.3 Summary

This chapter presents the literature relevant to this research. This includes experimented designs used to find the best configurations and determine which factors are significant. The next chapter will discuss the methodology of this research.

III. Methodology

3.1 Introduction of the Bootstrap

Statistics is the science of learning from experience, especially experience that arrives a little bit at a time (7). Statistical theory provides sound methods for finding a real signal in a noisy background while providing strict checks against the over-interpretation of random patterns.

Statistical theory attempts to give answer three basic questions:

- How should one collect data?
- How should one analyze and summarize the data collected?
- How accurate are the data summaries?

The last question constitutes the part of the process known as statistical inference.

Several modern methods of what is often called *computer-intensive statistics* make use of extensive repeated calculations to explore the sampling distribution of a parameter estimator $\hat{\theta}$. The bootstrap is a recently developed technique for making certain kinds of statistical inference using modern computer power to simplify the often intricate calculations of traditional statistical theory (7). It is only recently developed because it requires a modern powerful computer to execute the often intricate calculations of traditional statistical theory. The explanations for the bootstrap method involve explanations of traditional ideas in statistical inference. The basic ideas of statistics have not changed, but their implementation has. The modern powerful computer can apply these ideas flexibly, quickly, easily, and with a minimum of mathematical assumptions. The primary purpose of this chapter is to explain the basic ideas of bootstrap method and how it is applied in this research.

3.2 Basic Ideas of the Bootstrap

The bootstrap is a computer-based method for assigning measures of accuracy to statistical estimates (7). As with other methods of statistical inference, the bootstrap method makes use of a sample. While the usual assumption is that the sample is a collection of independent entities from the same distribution, the central idea behind the bootstrap is to let *the sample play the role of the population.* The same functional of the distribution function of the sample should then be a good estimate of the parameter. The objective in using a bootstrap method is to estimate some parameter of a distribution, or to perform a test of a hypothesis about the parameter. A parameter of a population is a functional of the distribution function, F; for example, the mean

$$\mu = \int x \, dF(x), \tag{3.1}$$

or the variance

$$\sigma^2 = \int (x - \mu)^2 \, dF(x). \tag{3.2}$$

In general, it can be written both as a real-valued functional and as the value of the functional; i.e.,

$$\theta = \theta(F). \tag{3.3}$$

Other methods of statistical inference arise from this same idea. For instance, estimating a first moment (the mean) of a population uses the sample first moment. By letting the sample play the role of the population, the distribution function for the sample is the *empirical distribution function.* Because it corresponds to the population distribution function F we will denote it by $\hat{F}$ or sometimes by $\hat{F}_n$ to emphasize that it relies on a sample of size n. It can be formed from the discrete probability density function that puts mass $1/n$ at each point in the sample of size n.

A bootstrap statistic corresponding to $\theta = \theta(F)$ is

$$\hat{\theta} = \theta(\hat{F}) \tag{3.4}$$

and the mean, for example, would be

$$\hat{\mu} = \int x \, d\hat{F}(x). \tag{3.5}$$

A *bootstrap sample* $\mathbf{x}^* = (x_1^*, x_2^*, x_3^*, \cdots, x_n^*)$ is obtained from $\hat{F}$ by randomly sampling n times, with replacement, from the original data points $x_1, x_2, \cdots, x_n$ (7).

$$\hat{F} \longrightarrow (x_1^*, x_2^*, \cdots, x_n^*). \tag{3.6}$$

The star notation indicates that $\mathbf{x}^*$ is not the actual data set $\mathbf{x}$, but rather a randomized, or *resampled*, version of $\mathbf{x}$. Thus, the bootstrap data points $x_1^*, x_2^*, \cdots, x_n^*$ are chosen independently and with equal probability from the sample. The bootstrap data set $(x_1^*, x_2^*, \cdots, x_n^*)$ consists of members of the original data set $(x_1, x_2, \cdots, x_n)$ where some values appear zero times, others once, twice, etc. For instance, with n=10 there is a finite probability of finding $\mathbf{x}^* = (x_3, x_8, x_1, x_5, x_9, x_3, x_4, x_1, x_5, x_2)$.

Figure 3.1 is a schematic of the bootstrap process. The bootstrap algorithm begins by generating a large number B of independent bootstrap samples $\mathbf{x}^{*1}$, $\mathbf{x}^{*2}$, $\cdots$, $\mathbf{x}^{*B}$, each of size n (7).

3.3 The Bootstrap Estimate of Standard Error

Standard errors are measures of statistical accuracy, where the *estimated standard error* of a mean $\bar{x}$ based on n independent data points $x_1, x_2, \cdots, x_n$, $\bar{x} = \sum_{i=1}^{n} x_i/n$, is given by the formula

$$\frac{s}{\sqrt{n}} \tag{3.7}$$

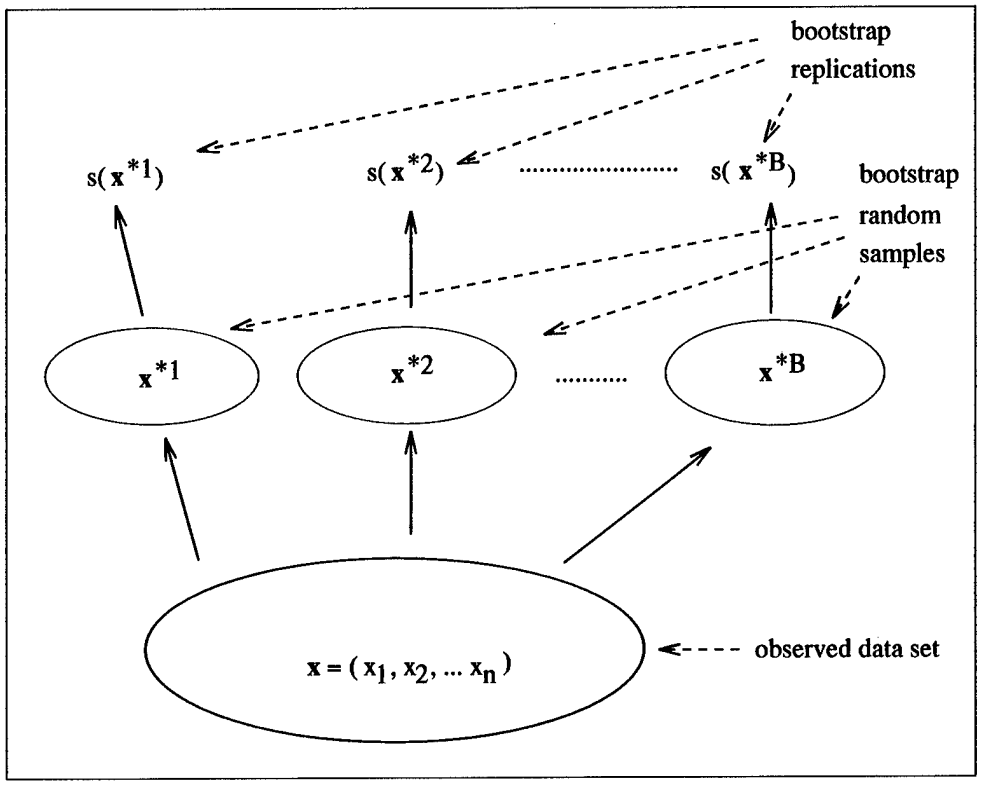

Figure 3.1 *Schematic diagram of the bootstrap process for estimating the standard error of a statistic* $s(\mathbf{x})$. *B bootstrap samples are generated from the original data set. Each bootstrap sample has n elements, generated by sampling with replacement n times from the original data set. Bootstrap replicates* $s(\mathbf{x}^{*1}), s(\mathbf{x}^{*2}), \cdots, s(\mathbf{x}^{*B})$ *are obtained by calculating the value of the statistic* $s(\mathbf{x})$ *on each bootstrap sample and they can be used to estimate the standard error of* $s(\mathbf{x})$ (Figure from *An Introduction to the Bootstrap* by Efron and Tibshirani (7)).

where $s = \sqrt{\sum_{i=1}^{n}(x_i - \bar{x})^2/(n-1)}$. Roughly speaking, an estimator will be less than one standard error away from its expectation about 68% of the time, and less than two standard errors away about 95% of the time due to the central limit theorem (CLT). (Typical values for B, the number of bootstrap samples, range from 50 to 200 for standard error estimation (7).) Corresponding to each bootstrap sample in Figure 3.1 is a *bootstrap replication* of s, namely $s(\mathbf{x}^{*m})$, the value of the statistic s evaluated for $\mathbf{x}^{*m}$. If $s(\mathbf{x})$ is the sample median, for instance, then $s(\mathbf{x}^*)$ is the

median of the bootstrap sample. The bootstrap estimate of standard error is the standard deviation of the bootstrap replications,

$$\widehat{\mathrm{se}}_{\mathrm{b}} = \{\sum_{m=1}^{B} [s(\mathbf{x}^{*m}) - s(\eta)]/(B-1)\}^{\frac{1}{2}}, \tag{3.8}$$

where $s(\eta) = \sum_{m=1}^{B} s(\mathbf{x}^{*m})/B$ (7). Suppose $s(\mathbf{x})$ is the mean $\bar{x}$. In this case, standard probability theory tells us that as B gets very large, formula (3.8) approaches

$$\{\sum_{i=1}^{n} (x_i - \bar{x})^2/n^2\}^{\frac{1}{2}} \tag{3.9}$$

This is almost the same as formula (3.7). We could make it exactly the same by multiplying formula (3.8) by the factor $[\sqrt{n/(n-1)}]$, but there is no real advantage in doing so since the factor approaches unity for large n.

Suppose that x is a real-valued random variable with an unknown probability distribution F. Let us denote the expectation and variance of F by the symbols μ_F and σ_F^2 respectively,

$$\mu_F = \mathtt{E}_F(x), \qquad \sigma_F^2 = \mathtt{var}_F(x) = \mathtt{E}_F[(x - \mu_F)^2]. \tag{3.10}$$

Here we are emphasizing the dependence on F. The alternative notation "$\mathrm{var}_F(x)$" for the variance, sometimes abbreviated to $\mathrm{var}(x)$, means the same thing as σ_F^2. In what follows we will sometimes write

$$x \sim (\mu_F, \sigma_F^2) \tag{3.11}$$

to indicate concisely the expectation and variance of random sample x.

Now let $(x_1, \cdots, , x_n)$ be a random sample of size n from the distribution F. The mean of the sample $\bar{x} = \sum_{i=1}^{n} x_i/n$ has expectation μ_F and variance σ_F^2/n; i.e.,

$$\bar{x} \sim (\mu_F, \sigma_F^2/n). \tag{3.12}$$

In other words, the expectation of $\bar{x}$ is the same as the expectation of a single x, but the variance of $\bar{x}$ is $1/n$ times the variance of x. The larger n is, the smaller $\mathrm{var}(\bar{x})$ is, so larger n yields a better estimate of μ_F.

The *standard error* of the sample mean $\bar{x}$, written $\mathrm{se}_F(\bar{x})$ or $\mathrm{se}(\bar{x})$, is the square root of the variance of $\bar{x}$,

$$\mathbf{se}_F(\bar{x}) = \sqrt{\mathbf{var}_F(\bar{x})} = \sqrt{\sigma_F^2/n}. \tag{3.13}$$

Under quite general conditions on F, the distribution of $\bar{x}$ will be approximately normal as n gets large due to the CLT, which we can write as

$$\bar{x} \sim N(\mu_F, \sigma_F^2/n). \tag{3.14}$$

The expectation μ_F and variance σ_F^2/n in (3.14) are exact, while the normality is approximate. A table of the normal distribution gives

$$\mathrm{P}\{|\,\bar{x} - \mu_F\,| < \sqrt{\frac{\sigma_F^2}{n}}\} \doteq 0.683 \qquad \mathrm{P}\{|\,\bar{x} - \mu_F\,| < 2\sqrt{\frac{\sigma_F^2}{n}}\} \doteq 0.954 \tag{3.15}$$

as illustrated in Figure 3.2. One of the advantages of the bootstrap method is that we do not have to depend entirely on the central limit theorem. Later we will see how to get accuracy statements like definition (3.15) directly from the data. It will then be clear that formula (3.15), which is correct for large values of n, can sometimes be quite inaccurate for the sample size actually available. Keeping this in mind, it is still true that the standard error of an estimate usually gives a good idea of its accuracy.

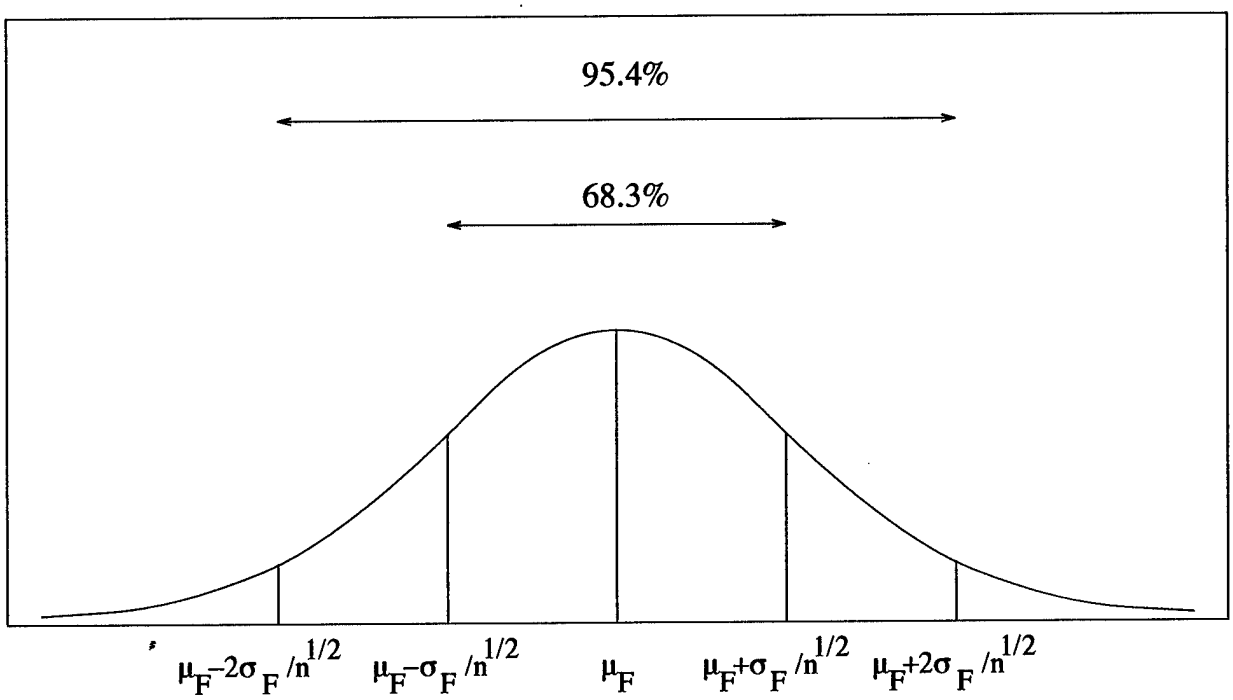

Figure 3.2 *For large values of n, the mean $\bar{x}$ of a random sample from F will have an approximate normal distribution with mean μ_F and variance σ_F^2/n* (from *An Introduction to the Bootstrap* by Efron and Tibshirani (7)).

Suppose we find ourselves in the following common data-analytic situation: a random sample $\mathbf{x} = (x_1, x_2, \cdots, x_n)$ from an unknown probability distribution F has been observed and we want to estimate a parameter of interest $\theta = t(F)$ on the basis of $\mathbf{x}$. For this purpose, we calculate an estimate $\hat{\theta} = s(\mathbf{x})$ from $\mathbf{x}$.

Algorithm 3.1 is a more explicit description of the bootstrap procedure for estimating the standard error of $\hat{\theta}$ from the observed data $\mathbf{x}$.

Bootstrap Algorithm for Estimating Standard Errors

1. Select a large number B of independent bootstrap samples $\mathbf{x}^{*1}, \mathbf{x}^{*2}, \cdots, \mathbf{x}^{*B}$, each consisting of n data values drawn with replacement from observed data set $\mathbf{x}$, as in (3.6).

2. Evaluate the bootstrap mean corresponding to each bootstrap sample,

$$\hat{\theta}^*(m) = s(\mathbf{x}^{*m}) \quad m = 1, 2, \cdots, B$$

3. Estimate the standard error $se_F(\hat{\theta})$ by the sample standard deviation of the B replications

$$\widehat{\text{se}}_{\text{b}} = \sqrt{\textstyle\sum_{m=1}^{B} [\hat{\theta}^*(m) - \hat{\theta}^*(\eta)]^2/(B-1)}\ ,$$

where $\hat{\theta}^*(\eta) = \sum_{m=1}^{B} \hat{\theta}^*(m)/B$.

Algorithm 3.1 (Based on an idea from (7)).

Figure 3.3 is a schematic diagram of the bootstrap procedure as it applies to one-sample situations. On the left is the real world, where an unknown distribution F has given the observed data $\mathbf{x} = (x_1, x_2, \cdots, x_n)$ by random sampling. We have calculated a statistic of interest from $\mathbf{x}$, $\hat{\theta} = s(\mathbf{x})$, and wish to know something about $\hat{\theta}$'s statistical behavior, perhaps its standard error $\text{se}_F(\hat{\theta})$. On the right side of the diagram is the bootstrap world. In the bootstrap world, the empirical distribution $\hat{F}$ gives bootstrap samples $\mathbf{x} = (x_1^*, x_2^*, \cdots, x_n^*)$ by random sampling with replacement,

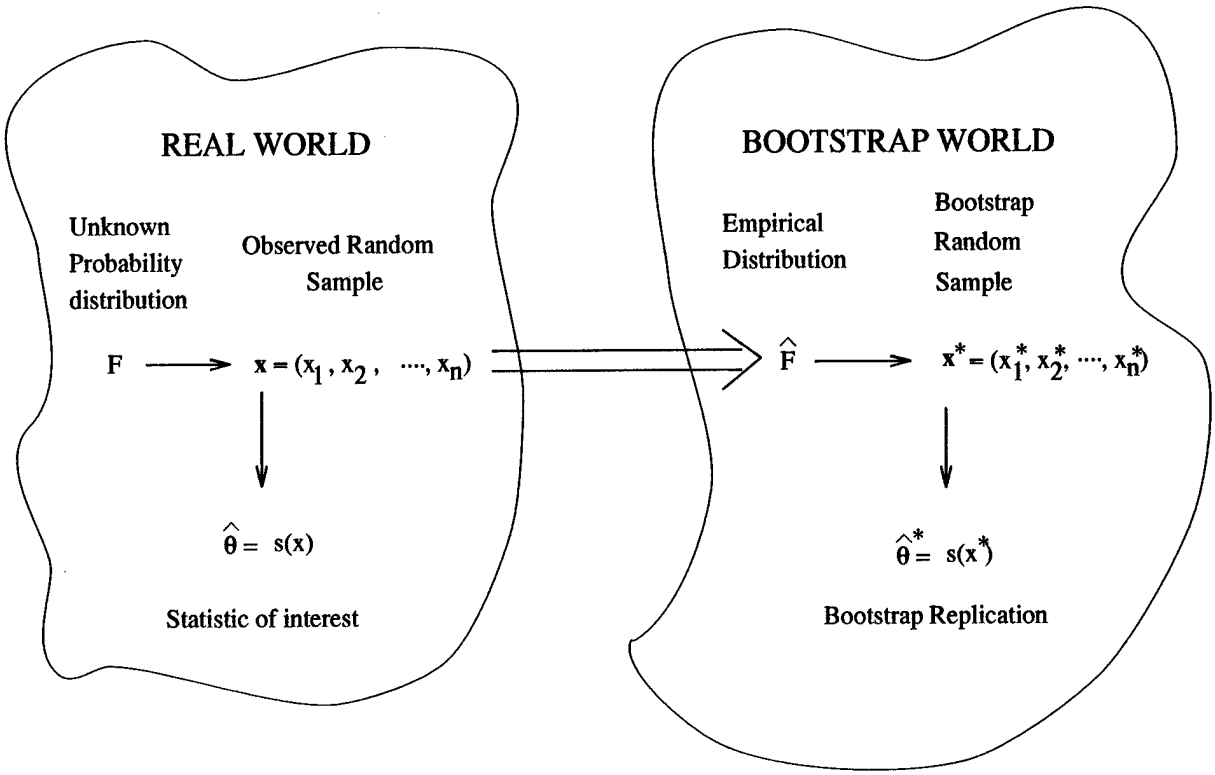

Figure 3.3 *A schematic diagram of the bootstrap which it applies to one-sample problems* (from *An Introduction to the Bootstrap* by Efron and Tibshirani (7)).

from which we calculate bootstrap replications of the statistic of interest, $\hat{\theta}^* = s(\mathbf{x}^*)$. The advantage of the bootstrap world is that we can calculate as many replications of $\hat{\theta}^*$ as we want. This allows us to do probabilistic calculations directly - for example, using the observed variability of the $\hat{\theta}^*$'s to estimate the unobservable quantity $\text{se}_F(\hat{\theta})$.

Furthermore, it can simply be applied to general data structure by replace F to D. There is not much conceptual difference between the two definitions, except for the level of generality involved. In the real world, an unknown probability distribution D gives an observed random sample data set $\mathbf{x}$. In the general data structure, the bootstrap world side is defined by analogous quantities in the real world. The

arrow in $\hat{D} \rightarrow \mathbf{x}^*$ is defined to mean the same way as the arrow $D \rightarrow \mathbf{x}$, while the function mapping $\mathbf{x}^*$ to $\hat{\theta}^*$ is the same function $s(\eta)$ as from $\mathbf{x}$ to $\hat{\theta}$.

3.4 The Bootstrap Confidence Interval

3.4.1 Introduction. The objective of statistics is to make an inference about a population based on information contained in a sample (16). Because populations are characterized by numerical descriptive measures called *parameters*, the objective of many statistical investigations is to make an inference about one or more population parameters. Most statistical inference procedures involve either estimation or hypothesis testing. An interval estimator is a rule that specifies the method for using the sample measurements to calculate two numbers that form the endpoints of the interval (16). Interval estimators are called *confidence intervals*, and the upper and lower endpoints of a confidence interval are called the *upper* and *lower confidence limits*, respectively. Standard errors are often used to assign approximate confidence intervals to a parameter θ and an estimated standard error $\hat{se}$; i.e., the usual 90% confidence interval for θ is

$$\hat{\theta} \pm 1.645 \cdot \hat{se} \tag{3.16}$$

with the constant value 1.645 coming from a standard normal table. Formula 3.16 is called an *interval estimate* or *confidence interval* for θ. Taken together, the point estimate and the interval estimate say what is the best guess for θ, and how far in error that guess might reasonably be (7).

The bootstrap procedure for generating confidence bands for a parameter, estimated by a statistic that is a function of n independent and identically distributed (iid) observations, may be summarized as follows. Obtain the empirical distribution of the statistic from m independent samples of size n generated with the empirical distribution of the original n observations. For sufficiently large m, one thus obtains an arbitrarily good approximation to a distribution that in itself is a good estimate

of the true distribution of the statistic. Suppose that we are in the one-sample situation where the data are obtained by random sampling from an unknown distribution F, $F \to \mathbf{x} = (x_1, x_2, \cdots, x_n)$. Let $\hat{\theta} = t(\hat{F})$ be the estimate of a parameter of interest $\theta = t(F)$, and let $\widehat{\text{se}}$ be some reasonable estimate of standard error for $\hat{\theta}$, based perhaps on bootstrap computations. Under most circumstances it turns out that as the sample size n grows large, the distribution of $\hat{\theta}$ becomes more and more normal, with mean near θ and variance near $\widehat{\text{se}}^2$, written $\hat{\theta} \dot{\sim} N(\theta, \widehat{\text{se}}^2)$ or equivalently

$$\frac{\hat{\theta} - \theta}{\widehat{\text{se}}} \dot{\sim} N(0,1). \tag{3.17}$$

The *large-sample* result (3.17) usually holds true for general probability models $P \to \mathbf{x}$ as the amount of data gets large, and for statistics other than the plug-in estimate (7).

Let z_α indicate the $100{\cdot}\alpha$th percentile point of a $N(0,1)$ standard normal distribution, as given in a standard normal table. Since $z_{(1-\alpha)} = -z_\alpha$, if we take approximation (3.17) to be exact, then

$$\text{P}_F\{z_\alpha \leq \frac{\hat{\theta} - \theta}{\widehat{\text{se}}} \leq z_{(1-\alpha)}\} = 1 - 2\alpha, \tag{3.18}$$

or equivalently

$$\text{P}_F\{\hat{\theta} - z_{(1-\alpha)} \cdot \widehat{\text{se}} \leq \theta \leq \hat{\theta} - z_\alpha \cdot \widehat{\text{se}}\} = 1 - 2\alpha, \tag{3.19}$$

where $\hat{\theta}$ is the maximum likelihood estimate (MLE) of θ, and $\widehat{\text{se}}$ is an estimate of its standard deviation.

In general

$$[\hat{\theta} - z_{(1-\alpha)} \cdot \widehat{\text{se}}, \hat{\theta} - z_\alpha \cdot \widehat{\text{se}}] \tag{3.20}$$

is called the *standard confidence interval* with confidence level $100{\cdot}(1 - 2\alpha)\%$. Or, more simply, it is called a 1-2α confidence interval for θ. We can restate (3.20) in

the more familiar form

$$\hat{\theta} \pm z_{(1-\alpha)} \cdot \hat{\text{se}}. \tag{3.21}$$

3.4.2 Review the Logic of Confidence Interval. We, first,review the logic of confidence intervals, and what it means for a confidence interval to be *accurate.*

Suppose that we are in the situation where an estimator $\hat{\theta}$ is normally distributed with unknown expectation θ,

$$\hat{\theta} \sim N(\theta, se^2), \tag{3.22}$$

with the standard error "se" known. (There is no dot over the "$\sim$" sign since we are assuming that 3.22 holds exactly.) Then the random quantity equaling $(\hat{\theta} - \theta)/se$ has a standard normal distribution,

$$Z = \frac{\hat{\theta} - \theta}{se} \sim N(0,1). \tag{3.23}$$

For convenience we will denote confidence intervals by $[\hat{\theta}_L, \hat{\theta}_U]$. In this case we can see that the interval $[\hat{\theta} - z_{(1-\alpha)} \cdot \text{se}, \hat{\theta} - z_\alpha \cdot \text{se}]$ has probability exactly 1-2α of containing the true value of θ. More precisely, the probability that θ lies below the lower limit is exactly α, as is the probability that θ exceeds the upper limit,

$$\mathrm{P}_\theta\{\theta < \hat{\theta}_L\} = \alpha, \qquad \mathrm{P}_\theta\{\theta > \hat{\theta}_U\} = \alpha. \tag{3.24}$$

The fact that (3.24) holds for every possible value of θ is what we mean when we say that a (1-2α) confidence interval $(\hat{\theta}_L, \hat{\theta}_U)$ is accurate. It is important to remember that θ is a constant in probability statements (3.24), the random variables being $\hat{\theta}_L$ and $\hat{\theta}_U$.

There is another way to express the statement that $(\hat{\theta}_L, \hat{\theta}_U)$ is a 1-2α confidence interval for θ. Suppose that θ were equal to $\hat{\theta}_L$, say

$$\hat{\theta}^* \sim N(\hat{\theta}_L, se^2). \tag{3.25}$$

Here we have used $\hat{\theta}^*$ to denote the random variable, to avoid confusion with the observed estimate $\hat{\theta}$. The quantity $\hat{\theta}_L$ is considered to be fixed in (3.25), with only $\hat{\theta}^*$ being random. It is easy to see that the probability that $\hat{\theta}^*$ exceeds the actual estimate $\hat{\theta}$ is α,

$$\mathrm{P}_{\hat{\theta}_L}\{\hat{\theta}^* \geq \hat{\theta}\} = \alpha \tag{3.26}$$

and for any value of θ less than $\hat{\theta}_L$ we have

$$\mathrm{P}_{\theta}\{\hat{\theta}^* \geq \hat{\theta}\} < \alpha. \tag{3.27}$$

The probability calculation in (3.27) has $\hat{\theta}$ fixed at its observed value, and $\hat{\theta}^*$ random, $\hat{\theta}^* \sim N(\theta, \hat{\mathbf{se}})$, so for any value of θ greater than the upper limit $\hat{\theta}_U$

$$\mathrm{P}_{\theta}\{\hat{\theta}^* \leq \hat{\theta}\} < \alpha. \tag{3.28}$$

The logic of the confidence interval $(\hat{\theta}_L, \hat{\theta}_U)$ can be stated in terms of (3.27 - 3.28). We decide that values of the parameter θ less than $\hat{\theta}_L$ are implausible, since they give probability less than α of observing an estimate as large as the one actually seen (3.27). We decide that values of the parameter θ greater than $\hat{\theta}_U$ are implausible, since they give probability less than α of observing an estimate as small as the one actually seen (3.28) (7).

3.4.3 Bootstrap-t Interval. The standard intervals (3.19) are extremely useful in statistical practice because they can be applied in an automatic way to almost any parametric situation. As we have seen, the standard confidence interval

is derived from the assumption that

$$Z = \frac{\hat{\theta} - \theta}{se} \dot{\sim} N(0,1). \tag{3.29}$$

This is valid as $n \to \infty$, but is only an approximation for finite samples. For the case $\hat{\theta} = \bar{x}$, Gosset (1908) derived the better approximation

$$Z = \frac{\hat{\theta} - \theta}{\hat{\text{se}}} \dot{\sim} t_{(n-1)}. \tag{3.30}$$

where $t_{(n-1)}$ represents the Student's t-distribution on $n-1$ degrees of freedom. Using this approximation, the confidence interval is

$$[\hat{\theta} - t_{(1-\alpha),(n-1)} \cdot \hat{\text{se}},\ \hat{\theta} - t_{(\alpha),(n-1)} \cdot \hat{\text{se}}], \tag{3.31}$$

with $t_{(\alpha),(n-1)}$ denoting the αth percentile of the t-distribution on $n-1$ degree of freedom. Using the t-distribution does not adjust the confidence interval to account for skewness in the underlying population or other errors that can result when $\hat{\theta}$ is not the sample mean; however, the bootstrap-t interval adjusts for these errors (7).

Through the use of the bootstrap procedure we can obtain accurate intervals without having to make normal theory assumptions like (3.29). The bootstrap-t interval approach procedure estimates the distribution of Z directly from the data. The bootstrap table is built by generating B bootstrap samples, and then computing the bootstrap version of Z for each. The bootstrap table consists of the percentiles of these B values. Using the algorithm 3.1, we generate B bootstrap samples $\mathbf{x}^{*1}, \mathbf{x}^{*2}, \cdots, \mathbf{x}^{*B}$ and for each we compute

$$Z^*(b) = \frac{\hat{\theta}^*(b) - \hat{\theta}}{\hat{\text{se}}^*(b)}, \tag{3.32}$$

where $\hat{\theta}^*(b) = s(\mathbf{x}^{*b})$ is the value of $\hat{\theta}$ for the bootstrap sample $\mathbf{x}^{*b}$ and $\widehat{\text{se}}^*(b)$ is the estimated standard error of $\hat{\theta}^*$ for the bootstrap sample $\mathbf{x}^{*b}$. The αth percentile of $Z^*(b)$ is estimated by the value $\hat{t}_\alpha$ such that

$$\{Z^*(b) \leq \hat{t}_\alpha\}/B = \alpha. \tag{3.33}$$

For example, if $B = 1000$, the estimate of the 2.5% point is the 25th largest value of $Z^*(b)$ and the estimate of the 97.5% point is the 975th largest value of $Z^*(b)$. Therefore, the bootstrap-t confidence interval is

$$(\hat{\theta} - t_{(1-\alpha)} \cdot \widehat{\text{se}},\ \hat{\theta} - t_{(\alpha)} \cdot \widehat{\text{se}}). \tag{3.34}$$

This is suggested by the same logic that gave (3.31) from (3.30) (7).

The bootstrap-t confidence interval procedure is a useful and interesting generalization of the usual Student's t method. It is particularly applicable to location statistics like the sample mean. (A location statistic is one for which increasing each data value x_i by a constant c increases the statistic itself by c.) Other location statistics are the median, the trimmed mean, or a sample percentile.

Until now we have discussed one approach to bootstrap confidence intervals. Next, we describe another approach based on percentiles of the bootstrap distribution of a statistic.

3.4.4 Bootstrap Percentile Interval. Let $\hat{\theta}$ be the usual estimate of a parameter θ and $\widehat{\text{se}}$ its estimated standard error. Consider the standard normal confidence interval$[\hat{\theta} - z_{(1-\alpha)} \cdot \widehat{\text{se}},\ \hat{\theta} - z_\alpha \cdot \widehat{\text{se}}]$. The endpoints of this interval can be described in a way that is particularly convenient for bootstrap calculations. Let $\hat{\theta}^*$ indicate a random variable drawn from the distribution $N(\hat{\theta},\ \widehat{\text{se}}^2)$,

$$\hat{\theta}^* \sim N(\hat{\theta},\ \widehat{\text{se}}^2). \tag{3.35}$$

Then $\hat{\theta}_L = \hat{\theta} - z_{(1-\alpha)} \cdot \hat{\text{se}}$ and $\hat{\theta}_U = \hat{\theta} - z_\alpha \cdot \hat{\text{se}}$ are the 100αth and 100(1-α)th percentile of $\hat{\theta}^*$. Suppose we are in the general situation of Figure 3.3 (Note: replace F to D). A bootstrap data set $\mathbf{x}^*$ is generated according to $\hat{D} \rightarrow \mathbf{x}^*$, and bootstrap replications $\hat{\theta}^* = s(\mathbf{x}^*)$ are 1-2α percentile interval is defined by the α and 1-α percentiles of $\hat{H}$:

$$[\hat{\theta}_{PL}, \hat{\theta}_{PU}] = [\hat{H}_\alpha, \hat{H}_{(1-\alpha)}]. \tag{3.36}$$

Since by definition $\hat{D}_\alpha = \hat{\theta}^*_\alpha$, the $100 \cdot \alpha$th percentile of the bootstrap distribution, we can also write the percentile interval as

$$[\hat{\theta}_{PL}, \hat{\theta}_{PU}] = [\hat{\theta}_\alpha, \hat{\theta}_{(1-\alpha)}]. \tag{3.37}$$

Expressions (3.36) and (3.37) refer to the ideal bootstrap situation in which the number of bootstrap replications is infinite. In practice we must use some finite number B of replications. To proceed, we generate B independent bootstrap data sets $\mathbf{x}^{*1}, \mathbf{x}^{*2}, \cdots, \mathbf{x}^{*B}$ and calculate the bootstrap replications $\hat{\theta}^*(b) = s(\mathbf{x}^{*b})$, $b = 1$, $2, \cdots, B$. Let $\widehat{\theta(B)}^*_\alpha$ be the $100 \cdot \alpha$th empirical percentile of the $\hat{\theta}^*(b)$ values, that is, the $B \cdot \alpha$th value in the ordered list of the B replications of $\hat{\theta}^*$. So if $B = 1000$ and $\alpha = 0.05$, $\widehat{\theta(B)}^*_\alpha$ is the 50th ordered value of the replications.

3.4.5 Application of Bootstrap procedure. With this background we can apply the bootstrap procedure to this research. Using November C-141 parachute and jumper belt position data and C-17 parachute and jumper belt position data, we first calculate midpoint between parachute and jumper belt position. In the C-141 case, 19 jumpers went out from the left door and 20 jumper's from the right. In the C-17 case, 20 jumpers exited from both the left door and right door. Thus, we know that there are 380 (19×20) possible left and right jumper pairs for the C-141 and 400 (20×20) pairs for the C-17. Second, we calculate minimum distance between each left jumper and right jumper pair at a time difference from -0.5 to 0.5 seconds

by 0.05 increments (-.5, -.45, -.40, $\cdots\cdots$, .40, .45, .5) – in effect, we discretize the continuous distribution. Thus, for the C-141 we get 7980 ($19 \times 20 \times 21$) minimum distances based on 21 different time intervals for each of the 380 possible pairs.

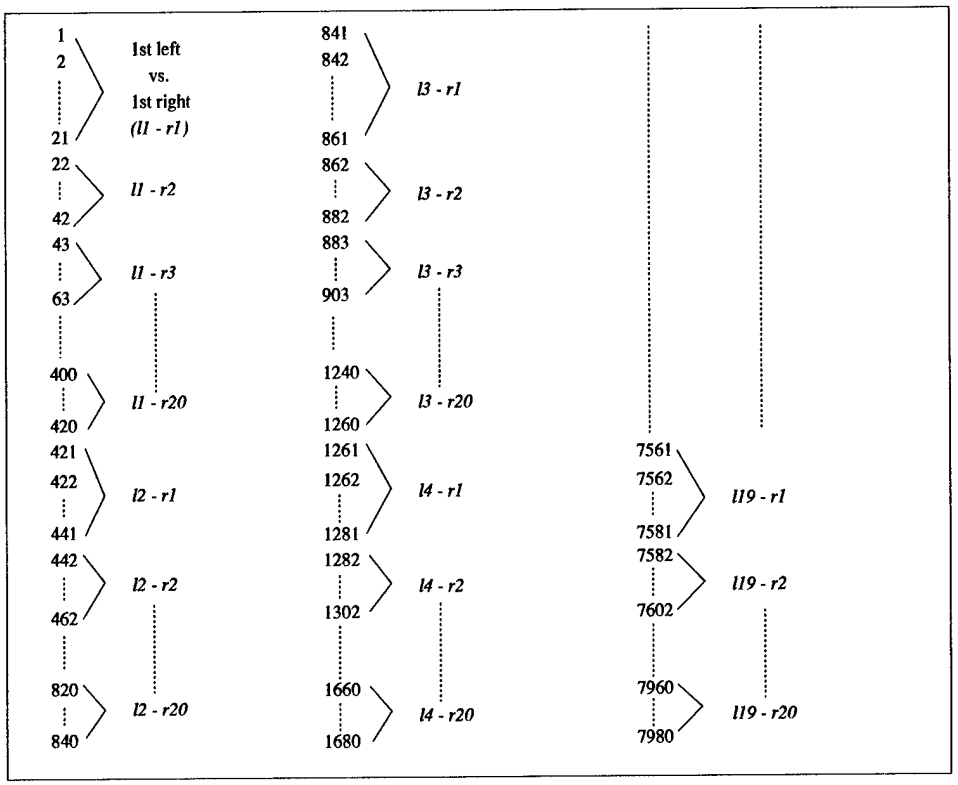

Figure 3.4 7980 Minimum distances of 19 left and 20 right jumper possible pairs in the November C-141.

The algorithm in Table 3.1 shows the procedure for generating the bootstrap replications of the November 1995 C-141 data. Figure 3.4 gives 7980 minimum distance as original data. Then, we generate all 1000 bootstrap samples by randomly selecting with replacement 19 left jumper and 20 right jumper distance sets using S-plus, Fortran, or other math or statistic programs. For example, we generate

$B^*_{l1} = \{14, 18, 11, 14, 12, 9, 3, 19, 14, 4, 5, 8, 11, 3, 14, 2, 13, 10, 1\}$,

$B^*_{l2} = \{12, 18, 5, 18, 2, 19, 9, 18, 12, 15, 17, 4, 14, 17, 3, 6, 7, 15, 6\}$

$\vdots$

$B^*_{l1000} = \{17, 12, 5, 14, 16, 1, 6, 18, 13, 7, 4, 6, 1, 6, 12, 6, 2, 14, 15\}$

Algorithm for Bootstrap Procedure

1. Using the original data, calculate j=(21×number of left×number of right) minimum distances (Figure 3.4) using Algorithm for Calculating Minimum Distances (Table 4.3).

2. Produce the sampling arrays B^*_{li} and B^*_{ri} ($i = 1000$) of size left and right jumpers, respectively, using replacement sampling. Set $i = 1$.

3. Using the ith sample arrays B^*_{li} and B^*_{ri} get the minimum distance from corresponding minimum distance set (Figure 3.4)

4. Sort this bootstrap sample in ascending order of the minimum distance and save as ith column.

5. Set $i = i + 1$. If $i \leq 1000$ go to step 3.

6. Sort rows 1 through i in ascending order.

7. Select columns by confidence interval.

Table 3.1 Algorithm for generating the 1000 independent Bootstrap Replications of the November 1995 C-141.

and

$B^*_{r1} = \{9, 1, 2, 11, 20, 3, 4, 10, 13, 14, 3, 12, 8, 4, 16, 1, 7, 19, 18, 6\}$

$B^*_{r2} = \{20, 10, 18, 20, 10, 7, 16, 16, 4, 19, 19, 1, 20, 5, 18, 14, 14, 7, 17, 20\}$

$\vdots$

$B^*_{r1000} = \{16, 6, 15, 12, 14, 4, 7, 8, 12, 18, 9, 1, 16, 13, 13, 13, 17, 20, 15, 3\}$

Using the bootstrap procedure, we generate 7980 minimum distances of the first bootstrap iteration with B^*_{l1} and B^*_{r1} by choosing matched 21 minimum distances from the original data in Figure 3.4. This procedure repeats until generating the 7980 minimum distances of the 1000th bootstrap iteration with B^*_{l1000} and B^*_{r1000}. Visualizing the results in a 7980 by 1000 matrix, each column represents 7980 minimum distances of each bootstrap iteration. After generating minimum distances of each bootstrap iteration, we then sort these minimum distances in ascending order for each column 1 - 1000. We sort again on rows 1 - 7980 by ascending order. After this sort, we then select 25th and 975th columns as 95% bootstrap confidence bounds, and plot the cumulative density function using these two columns. (Note: 50th and 950th, 100th and 900th, and 150th and 850th columns are 90%, 80%, and 70% bootstrap confidence lower and upper bounds, respectively.) Figure 3.5 shows 95% bootstrap confidence lower and upper bound of the November 1995 C-141 data. It should be pointed out that by calculating all minimum distances on the range of +.5 to -.5 second separation between left and right jumpers, the measurable outcome is the *worst case* minimum distance. An alternative approach would uniformly sample the +.5 to -.5 second separation interval to calculate the *expected* minimum distance; however, the U.S. Army preferred the former method.

3.4.6 Summary. In this section we discuss bootstrap procedure and how it applies to this research. In the next chapter, we discuss data analysis of the November C-141[1] versus November, March, and March-heavy C-17 data, and show

[1]This is the base line of this research for comparing to the C-17.

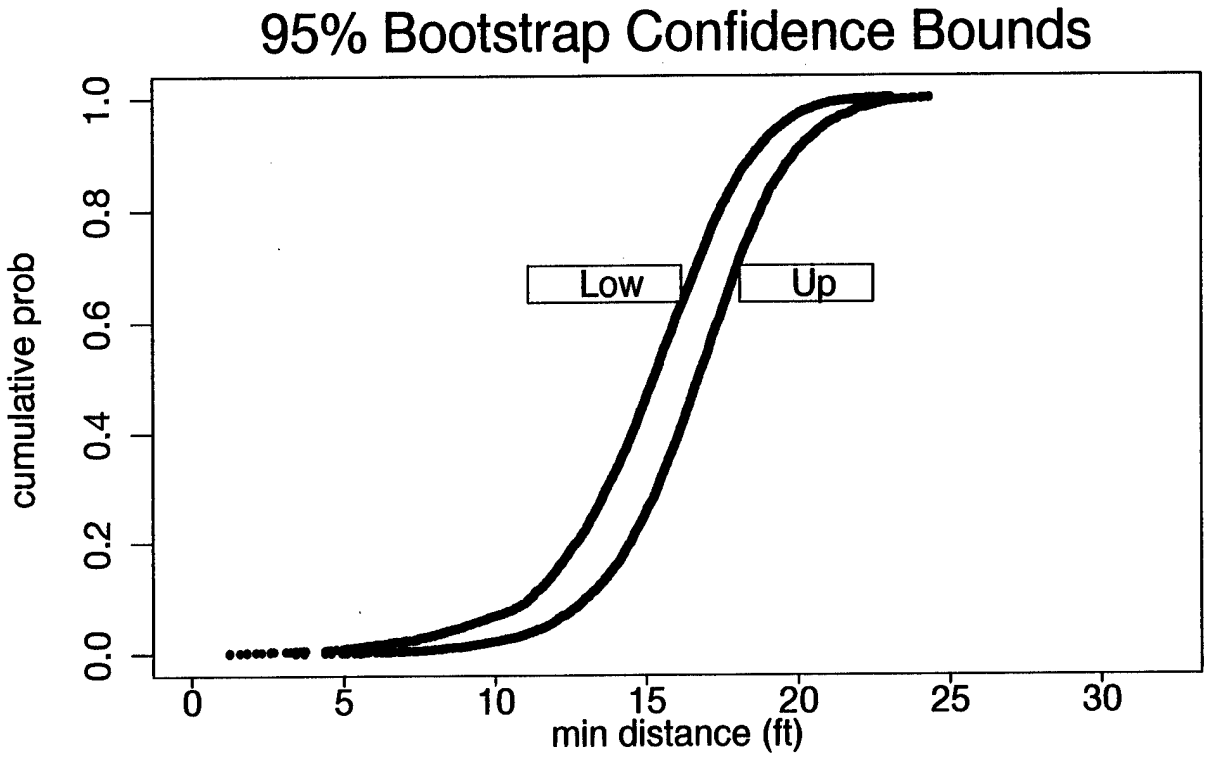

Figure 3.5 95% bootstrap confidence lower and upper bound of the November C-141.

the C-17 having a lower probability of entanglement than the C-141 by plotting bootstrap confidence bounds.

IV. An Analysis of the Experiment Data

4.1 Background

4.1.1 Data Source. The data which is used for this analysis can be obtained from several systems. We must first decide which data source to use, each presenting distinct advantages. As mentioned in Section 2.2.4, the CINE-T system at Edwards AFB was used to obtain data for the C-141 and C-17 baseline, and the reconfigured C-17. This system is limited to one jumper per pass but can be used to track both the body and the chute apex, thus allowing the computation of a centroid of the combined jumper-chute configuration. The Kineto Track Mount[1] (KTM) at Yuma and Fort Bragg is also limited to one jumper per pass. Both systems require good weather conditions; however, the weather conditions are usually better than Edwards and the co-located Army jumper unit at Yuma gives that KTM system cost and location benefits. The Airborne Space Positioning[2] (ASP) automatically tracks a single object, but offers the possibility of more than one object to be tracked in a single pass. The turn-around time for CINE-T is 10 - 14 days, but the accuracy is equivalent to that of the Personnel Airdrop Optimization (PAO) I (5 to 6 cameras). KTM and ASP would need to be assessed for accuracy, with new baselines established if one of these alternate systems were used. The KTM system offers 2-day turn-around (Yuma), while ASP has 8 to 24 hour turn-around. The CINE-T data can be adjusted for wind using software written by McDonnell Douglas, although under most conditions the families of trajectories change very little after adjustment with the later version of this software. Since KTM data has the same format as CINE-T, this data could also be adjusted for wind effects if deemed necessary. In this research I use four data sets (November 1994 C-141, November 1994 C-17, March 1995 C-17 and March 1995 heavy C-17). Even though the KTM (Yuma) has cost

[1]The brand name for a ground based trajectory tracking system similar to CINE-T, KTM uses video instead of film.

[2]Similar to CINE-T, but uses aircraft-mounted video cameras instead of movie cameras.

and location benefits, the CINE-T's accuracy provides a greater advantage. Table 4.1 shows configurations of each data set.

Factor	Nov 94 C-141	Nov 94 C-17	Mar 95 C-17	Mar 95 hC-17
Aircraft Speed	130 knots	135 knots	130 knots	130knots
Deck Angle	2°	2°	7°	7°
Gross Weight	330 – 360K	330 – 360K	330 – 360K	350 – 380K
Landing Gear	Up	Up	Up	Up
Static Line	15′	15′	15′	15′
Exit Style	45°	45°	45°	45°

Table 4.1 Configurations of November 1994 C-141, November 1994 C-17, March 1995 C-17, and March 1995 heavy C-17.

4.1.2 Data Form. Since the single data files of the four data set range from 460,000 to 1,000,000 bytes in size, we can not reasonably include the raw data in this paper[3]. However, to help understand the data analysis procedure, Table 4.2[4] presents a sample of the content of the CINE-T data.

In order to use the raw data file in the Table 4.2, we need ELAPS time (from when a jumper exits out from the aircraft door), XSM, YSM, and ZSM (which corresponds to the X, Y, and Z position value detailed in Chapter II). There are two columns which we have to consider in the Table 4.2. One is the third column (ELAPS), the other column five (YSM). Zero ELAPS time represents the left or right jumper exit out from the aircraft door. If ELAPS time value is negative (Index 1 to 56), it means the jumper has not yet exited. Therefore, in this case, we do not use the data from index 1 to index 56 since they are just waiting values. Index 57, where the ELAPS time is zero and Y-value is negative, indicates this data file is for right jumper since we assume positive Y is off the left wing. As mentioned in Chapter III, there are 19 left and 20 right jumpers; therefore, we can get files of 19

[3]All data set in Table 4.1 would require more than 1000 pages.
[4]Table 4.2 shows only one jumper's chute position values.

INDEX	HMS	ELAPS	XSM	YSM	ZSM	SECS
1.	153503.	-2.8	-548.7279	-2.7183	-7.3093	56103.
2.	153503.05	-2.75	-537.8914	-2.6989	-7.3866	56103.05
3.	153503.1	-2.7	-527.0763	-2.6656	-7.3606	56103.1
4.	153503.15	-2.65	-516.3075	-2.6066	-7.2129	56103.15
5.	153503.2	-2.6	-505.6069	-2.5451	-7.0279	56103.2
6.	153503.25	-2.55	-494.9438	-2.5242	-6.9196	56103.25
7.	153503.3	-2.5	-484.2321	-2.539	-6.9226	56103.3
⋮	⋮	⋮	⋮	⋮	⋮	⋮
55.	153505.7	-.1	29.6077	-7.0048	-4.8175	56105.7
56.	153505.75	-.05	40.3143	-7.2243	-5.0583	56105.75
57.	**153505.8**	**0.**	**51.0791**	**-7.321**	**-5.2729**	**56105.8**
58.	153505.85	.05	61.7647	-7.478	-5.5057	56105.85
59.	153505.9	.1	72.2758	-7.7535	-5.8945	56105.9
60.	153505.95	.15	82.5968	-8.099	-6.3505	56105.95
61.	153506.	.2	92.7835	-8.4493	-6.7382	56106.
⋮	⋮	⋮	⋮	⋮	⋮	⋮
195.	153512.7	6.9	435.3648	-24.9079	-158.6976	56112.7
196.	153512.75	6.95	434.2697	-25.1097	-159.4688	56112.75
197.	153512.8	7.	433.1223	-25.5052	-160.2765	56112.8
198.	153512.85	7.05	431.8921	-26.1185	-161.1653	56112.85
199.	153512.9	7.1	430.5896	-26.8858	-162.0548	56112.9
200.	153512.95	7.15	429.2006	-27.7265	-162.7805	56112.95
201.	153513.	7.2	427.7265	-28.5685	-163.2772	56113.

Table 4.2 The first right jumper's chute data form of the November C-141.

left jumper's chute and belt position values, and 20 right jumper's chute and belt position values[5].

4.1.3 Jumper Interval Distribution. In a mass jump, the objective is to jump from both side doors while maintaining an opposite door stagger. The time interval between same side jumpers is, on average, the total time to get n jumpers out, divided by $n-1$. We define Δt as the time interval between a given left jumper and his closest neighbor (before or after him) from the opposite side. We assume

[5]During the test, 20 jumpers jump out from each door, but one left jumper's trajectory was lost.

that Δt directly affects the distance traveled in the time interval between a pair of jumpers. (Note that the range on Δt is 0 to about half of the same side time interval.) For instance, the 10 Aug 1994 C-17 jump got 35 jumpers out in 43.945 seconds, so the average same side time interval is 43.945/34 = 1.29 seconds. Hence, we expect the range of Δt to be from 0 to about 0.65 seconds. While we desire Δt to be concentrated in the upper end of this range, the empirical data show a fairly uniform distribution between 0 to 0.65 seconds for both sides (13). Therefore, we maintain our assumption that the time interval between left and right jumper is uniformly distributed on the range -0.5 to 0.5 seconds.

4.2 Centerlining Tendency

To research a centerlining tendency of the airdrop procedure, we first calculate geometric midpoint values between each jumper's chute and belt position values (see Appendix A). Second, using these new midpoint values, we calculate the minimum distances on a range of time intervals between all possible pairs between left and right jumpers using the algorithm in Table 4.3 and Program 2 in Appendix B. Notionally, the procedure has the following properties:

- We treat the trajectory of each jumper as a sample trajectory (e.g., 19 left and 20 right jumpers give 39 sample trajectories).
- We make two major assumptions :
  - Any two trajectories (one left and one right) are equally likely to pair up as a *trajectory pair.*
  - For any *trajectory pair*, the time interval between the individual component trajectories commencing is uniformly distributed on the interval -.5 to .5 seconds.
- If we use .05 second time intervals, then for each possible left-right jumper combination we can simulate 21 paired trajectories, with each trajectory pair

Algorithm for Calculating Minimum Distances

step 1. L = 1, R = 1.

step 2. Calculate 21 minimum distances on Δt interval of -0.5 to +0.5 using Program 2 in Appendix B for trajectory pair LR.
Save the result to a file (refer to Figure 3.4).

step 3. R = R + 1.
If R > number of right jumpers go to step 4.
Otherwise go to step 2.

step 4. L = L + 1, R = 1.
If L > number of left jumpers stop.
Otherwise go to step 2.

Table 4.3 Algorithm for calculating the minimum distances of all possible trajectory pairs.

having a minimum distance between the two paired jumpers. (Note that the previous assumptions imply that the minimum distances of the 21 trajectory pairs is equally likely to occur.)

- Therefore, we can simulate $L \times R \times 21$ trajectory pairs, each providing a minimum distance. (In the case of the November 1994 C-17, the March 1995 C-17 (Gross weight 330 – 360 K), and the March 1995 heavy C-17 (Gross weight 350 – 380 K), we can get 8400, 8400, and 8379 minimum distances, respectively[6].)

In Table 4.3, step 2, we use the formula $\sqrt{(X_{li} - X_{rj})^2 + (Y_{li} - Y^*_{rj})^2 + (Z_{li} - Z_{rj})^2}$ to calculate the minimum distance, where

$$
\begin{aligned}
t &= \text{interval time on the range from -.5 to .5 seconds} \\
i &= \text{time after jumping out} \\
j &= i + t \\
X_{li} &= \text{left jumper } X \text{ position at time } i \\
X_{rj} &= \text{right jumper } X \text{ position at time } j \\
Y_{lj} &= \text{left jumper } Y \text{ position at time } i \\
Y_{rj} &= \text{right jumper } Y \text{ position at time } j \\
Y^*_{rj} &= Y_{rj} + (\text{aircraft speed} \times t)^7 \\
Z_{li} &= \text{left jumper } Z \text{ position at time } i \\
Z_{rj} &= \text{right jumper } Z \text{ position at time } j
\end{aligned}
$$

Figure 4.1 shows the results of the November 1994 C-141, the November 1994 C-17, the March 1995 C-17, and the March 1995 heavy gross weight C-17.

[6]In the cases of Nov 1994 C-17 and Mar 1995 C-17 (330 – 360 K), each side has 20 jumpers. Mar 1995 heavy C-17 produces 21 left jumpers and 19 right jumpers.

[7]this is adjusted by aircraft speed since aircraft advance amount of speed × time interval.

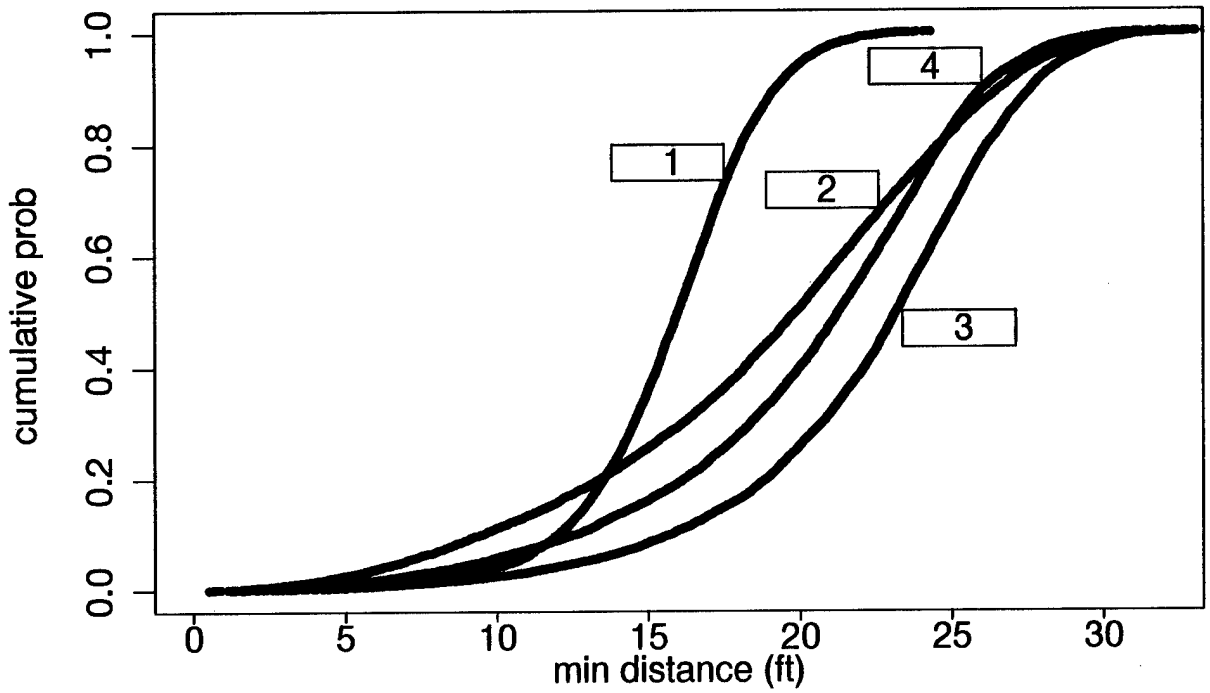

Figure 4.1 The base risk curves of airdrop tests; 1, 2, 3, and 4 show the risk curve of the November 1994 C-141, November 1994 C-17, March 1995 C-17, and the March 1995 heavy gross weight C-17, respectively.

4.3 Analysis

To analyze the data, we first need to generate N (in this research we use $N = 1000$) independent bootstrap samples by using the Algorithm in Table 3.1. Each bootstrap sample generates a column of K elements, so after repeating N times we get a $K \times N$ matrix $\mathbf{B}$ of minimum distances. We then sort the columns of $\mathbf{B}$ followed by a row sort using Fortran code in Appendix C. We then check original minimum distances and bootstrap median distances. Figure 4.2 shows comparison of original minimum distances and bootstrap median distances of each airdrop test. Since all plots are nearly equal, so we can use the bootstrap procedure for getting confidence intervals in this test. In Chapters II and III, we describe the bootstrap confidence interval, with particular interest in the idea of the bootstrap percentile

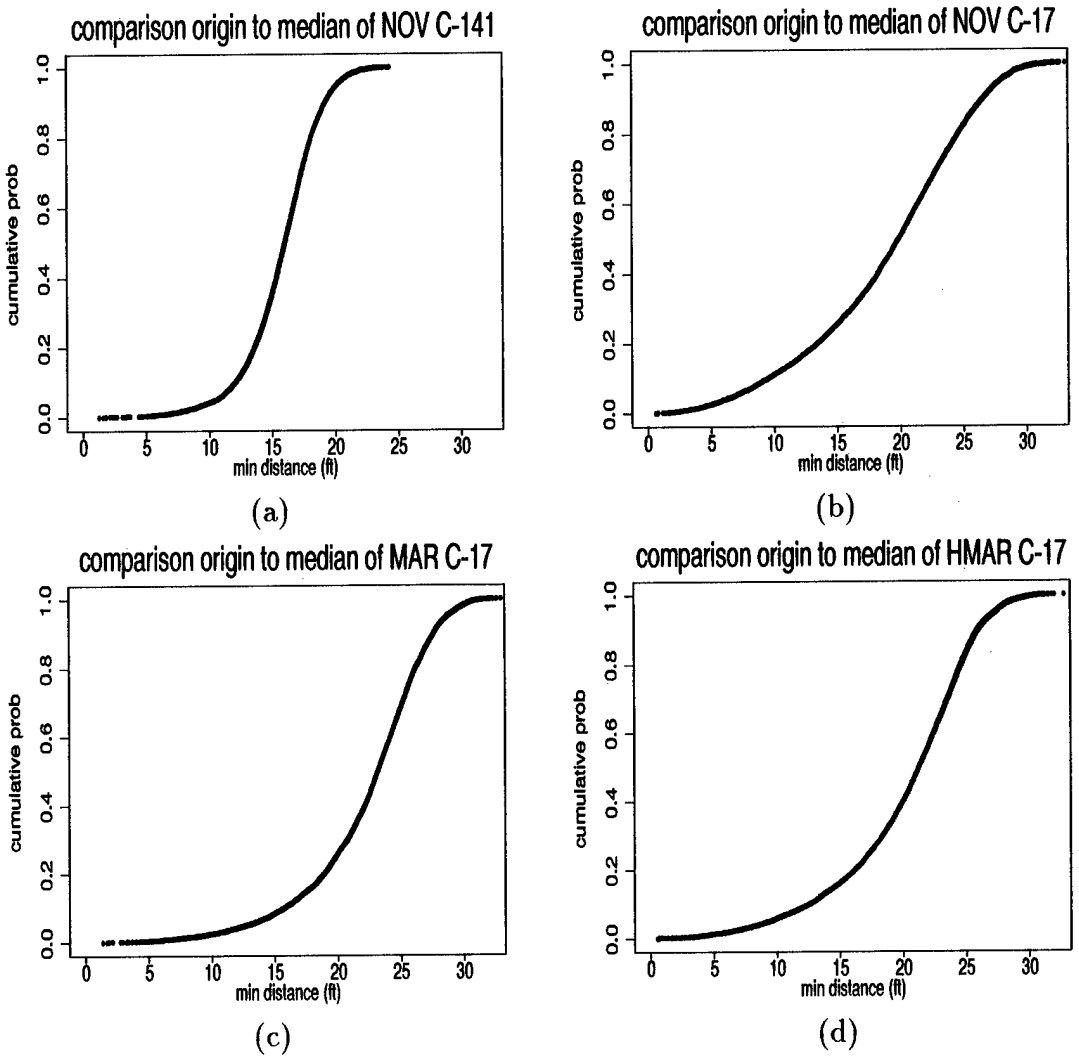

Figure 4.2 Comparing bootstrap median distance vs. original minimum distances of November 1994 C-141 (a), November 1994 C-17 (b), March 1995 C-17 (c), and heavy gross March 1995 C-17 (d).

interval (see Section 3.4.3). For instance, if we want a 95% bootstrap confidence bounds, we can select the columns matched N times $\alpha/2$ and N times (1 - $\alpha/2$) as lower and upper bound, respectively. In this case, N is 1000 and α is .05, thus the 25th column and the 975th column are selected as 95% bootstrap confidence lower and upper bound.

We plot these columns which matched each bootstrap confidence interval as a bootstrap confidence bounds, comparing the 95% and 50% bootstrap confidence bounds between November 1994 C-141 vs. November 1994 C-17 (Figure 4.3), November 1994 C-141 vs. March 1995 C-17 (Figure 4.4), and November 1994 C-141 vs. heavy gross weight March 1995 C-17 (Figure 4.5). We include the 50% bootstrap confidence interval at the Army's request. The 90%, 80%, 70%, and 60% bootstrap confidence bounds plots are in the Appendix D.

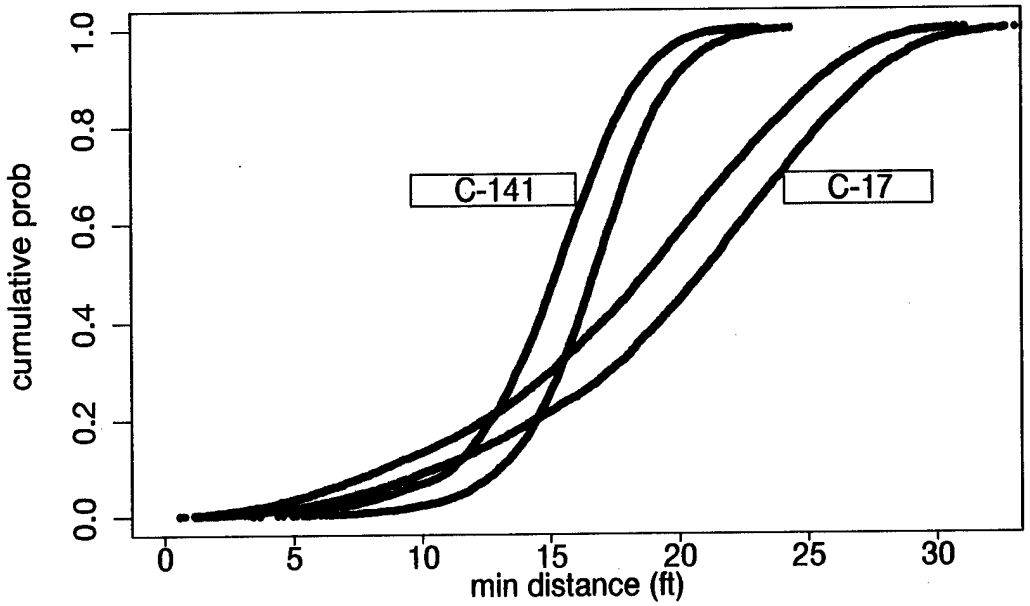

(a)

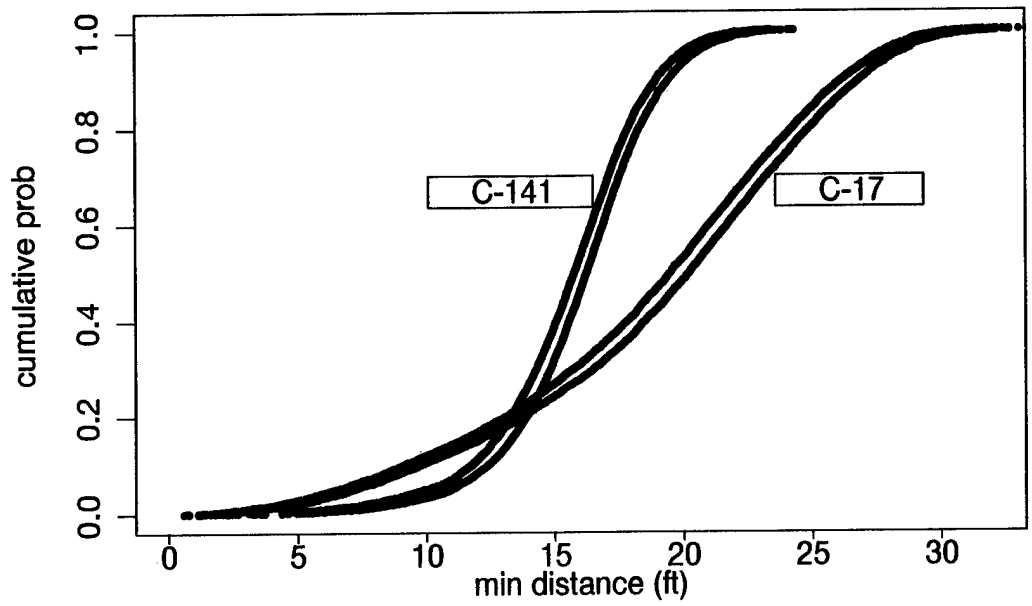

(b)

Figure 4.3 Comparing Bootstrap Confidence bounds between C-141 vs. November C-17: (a) 95% bootstrap confidence bounds (b) 50% bootstrap confidence bounds.

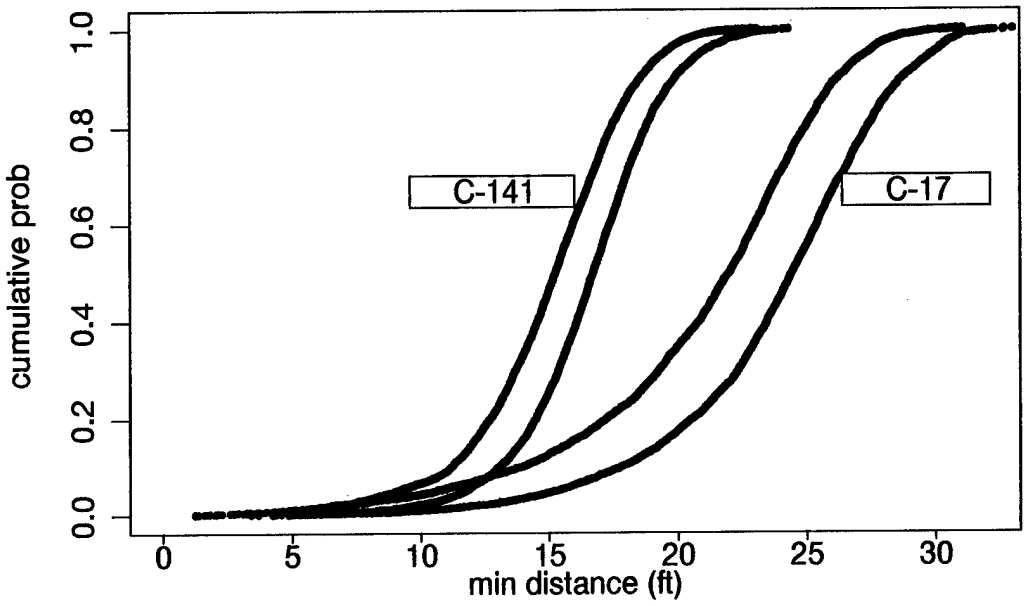

(a)

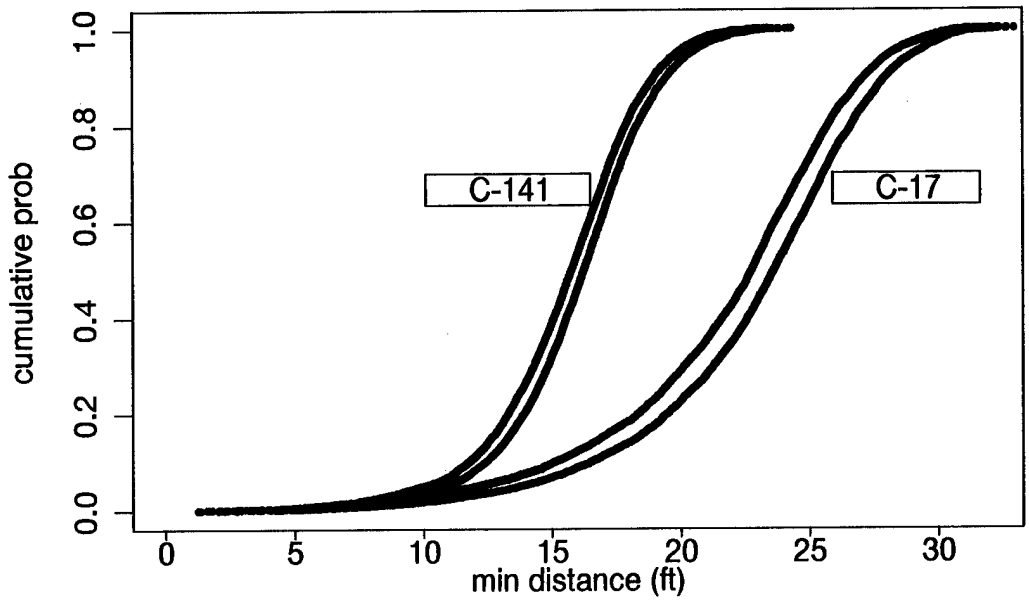

(b)

Figure 4.4 Comparing Bootstrap Confidence bounds between C-141 vs. March C-17: (a) 95% bootstrap confidence bounds (b) 50% bootstrap confidence bounds.

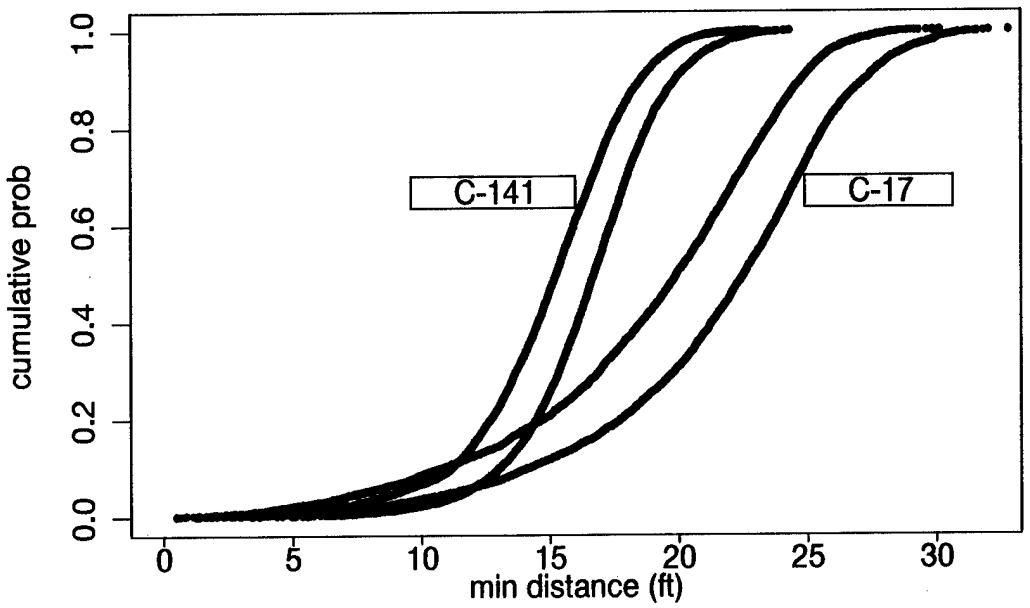

(a)

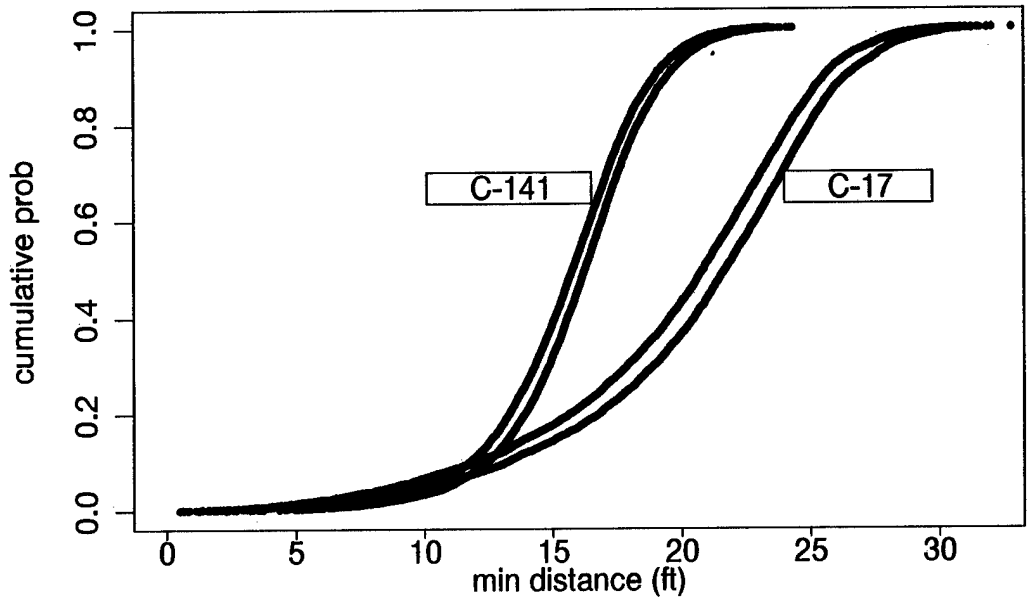

(b)

Figure 4.5 Comparing Bootstrap Confidence bounds between C-141 vs. March heavy C-17: (a) 95% bootstrap confidence bounds (b) 50% bootstrap confidence bounds.

4.4 Results

The results show that the March 1995 C-17 configuration meets or exceeds the November 1994 C-141 worst-case minimum separations. In Figure 4.3 (a) between 12 and 16 feet minimum distance the two confidence bounds are overlapping, so we can say that there is a strong evidence that the two systems are not different within that range. Conversely, no overlapping between 5 and 11 feet range gives strong evidence that the two systems are not the same ($P(S_{C-141} \leq d) < P(S_{C-17} \leq d)$). Comparisons below 5 feet given in Table 4.4 show $P(S_{C-141} \leq d) < P(S_{C-17} \leq d)$. Figure 4.3 (b) and Table 4.4, give similar results. After changing aircraft test configurations we get Figure 4.4 – 5. Since it is difficult to distinguish the plots below 10 ft, Tables 4.5 – 8 are provided.

Level	≤ 5	≤ 4	≤ 3	≤ 2	≤ 1
Low 95% C-141.Nov	0.815%	0.539%	0.301%	0.15%	0.075%
Up 95% C-17.Nov	1.607%	0.940%	0.476%	0.131%	0.024%
Low 50% C-141.Nov	0.439%	0.301%	0.138%	0.05%	0.025%
Up 50% C-17.Nov	2.202%	1.262%	0.702%	0.238%	0.095%

Table 4.4 Comparison the bootstrap confidence bounds between the November C-141 vs. the November C-17.

Table 4.9 is a summary of Figures 4.3 – 5 and Tables 4.4 – 8. For example, we can say $P(S_{C-17} \leq d) < P(S_{C-141} \leq d)$ above 15.6 ft minimum distance at the 95% and above 14.3 ft minimum distance at the 50% bootstrap confidence interval,

Level	≤ 10	≤ 8	≤ 6	≤ 4	≤ 2	≤ 1
Up 95% C-141.Nov	2.093%	0.702%	0.175%	0.025%	0.0%	0.0%
Low 95% C-17.Mar	4.321%	2.75%	1.452%	0.595%	0.131%	0.071%
Low 95% C-141.Nov	6.654%	3.296%	1.491%	0.539%	0.150%	0.0%
Up 95% C-17.Mar	0.833%	0.345%	0.119%	0.0%	0.0%	0.0%

Table 4.5 Comparison the 95% bootstrap confidence bounds between the November C-141 vs. the March.360 C-17.

Level	≤ 10	≤ 8	≤ 6	≤ 4	≤ 2	≤ 1
Up 50% C-141.Nov	3.246%	1.303%	0.451%	0.125%	0.0%	0.0%
Low 50% C-17.Mar	2.869%	1.679%	0.809%	0.286%	0.048%	0.024%
Low 50% C-141.Nov	4.900%	2.192%	0.877%	0.301%	0.05%	0.0%
Up 50% C-17.Mar	1.714%	0.857%	0.369%	0.071%	0.0%	0.0%

Table 4.6 Comparison the 50% bootstrap confidence bounds between the November C-141 vs. the March.360 C-17.

Level	≤ 10	≤ 8	≤ 6	≤ 4	≤ 2	≤ 1
Up 95% C-141.Nov	2.093%	0.702%	0.175%	0.025%	0.0%	0.0%
Low 95% hC-17.Mar	8.521%	5.215%	2.876%	1.217%	0.406%	0.298%
Low 95% C-141.Nov	6.654%	3.296%	1.491%	0.539%	0.150%	0.0%
Up 95% hC-17.Mar	3.533%	1.790%	0.847%	0.310%	0.048%	0.0%

Table 4.7 Comparison the 95% bootstrap confidence bounds between the November C-141 vs. the March.380 C-17.

Level	≤ 10	≤ 8	≤ 6	≤ 4	≤ 2	≤ 1
Up 50% C-141.Nov	3.246%	1.303%	0.451%	0.125%	0.0%	0.0%
Low 50% hC-17.Mar	6.599%	3.831%	2.065%	0.847%	0.251%	0.167%
Low 50% C-141.Nov	4.900%	2.192%	0.877%	0.301%	0.05%	0.0%
Up 50% hC-17.Mar	4.810%	2.661%	1.361%	0.513%	0.143%	0.023%

Table 4.8 Comparison the 50% bootstrap confidence bounds between the November C-141 vs. the March.380 C-17.

Aircraft Test Conditions	$P(S_{C-17} \leq d) < P(S_{C-141} \leq d)$		$P(S_{C-141} \leq d) < P(S_{C-17} \leq d)$	
	95%	50%	95%	50%
Nov 94 C-141 vs Nov 94 C-17	$d = 15.6$ ft	$d = 14.3$ ft	$d = 11.7$ ft	$d = 13.0$ ft
Nov 94 C-141 vs Mar 95 C-17	$d = 12.6$ ft	$d = 9.3$ ft	N/A	N/A
Nov 94 C-141 vs Mar 95 Heavy C-17	$d = 14.4$ ft	$d = 12.8$ ft	N/A	$d = 9.5$ ft

Table 4.9 Comparison the range of which system is better at 95% and 50% bootstrap confidence bounds.

but $P(S_{C-141} \leq d) < P(S_{C-17} \leq d)$ below 11.7 ft at the 95% and below 13.0 ft at the 50% bootstrap confidence intervals. In case of the March 1995 C-17, we can not distinguish the C-141 from the C-17 below 12.6 ft and 9.3 ft at 95% and 50% bootstrap confidence intervals, respectively, since the confidence bounds are overlapping. In the March heavy 1995 C-17 case, the two systems are not different below 14.4 ft minimum distance at the 95% bootstrap confidence interval; however, $P(S_{C-141} \leq d) < P(S_{C-17} \leq d)$ below 9.5 ft at the 50% bootstrap confidence interval.

V. Conclusions and Recommendations

5.1 Introduction

This Chapter summarizes the results of this research and makes recommendations for future efforts.

5.2 Results Summary

This research calculated the centerlining tendency of personnel airdrop of C-17 and C-141, compared the risk probability of both systems, and found where $P(S_{C-17} \leq d) < P(S_{C-141} \leq d)$ using the bootstrap method. From Table 4.9 in Chapter IV, the results show that the risk of entanglement for the C-17 can be controlled such that it is less than the C-141's. Under November 1994 configurations, $P(S_{C-141} \leq d) < P(S_{C-17} \leq d)$ when $d = 11.7$ ft (95%) and 13.0 ft (50%); i.e., the entanglement risk probability of the C-17 is higher than the C-141's at small distances. However, the March 1995 configurations show the probability of C-17 entanglement equal to or lower than the C-141's at small distances. This result is very important to both the C-17 SPO and U.S. Army for the following reason: *If the results showed that the risk probability of the C-17 is not less than the C-141's at any configuration, then the C-17 would be evaluated as not mission ready.* However, this analysis conclusively shows that – under certain configurations – the C-17 is as safe as the C-141 with respect to the risk of chute entanglement.

5.3 Suggestions for Future Research

First, additional research should be conducted in the future to eliminate the effects of these small sample sizes. For example, the data in this thesis uses a jumper sample size of 19 to 21; however, future research should use more jumpers. (For example, 51 jumpers exit out from each door per aircraft in operational airdrops.) Second, these curves are built under the measurable outcome of *worst case* scenarios

(i.e., smallest *possible* distances) between each pair of jumpers. Further analysis should introduce a uniform sampling of the left-right jumper exit times as a basis for simulating the *expected* outcome (i.e., average distances). Finally, this methodology should be applied to the deployment-bag strike problem.

Appendix A. Program 1

This Fortran program calculates midpoint values between each jumper's belt and helmet position.

```
C  DECLARE VARIABLE TYPES
INTEGER I
REAL XM, YM, ZM, XJ, XC, YJ, YC, ZJ, ZC
REAL XD, DIST, TI, TT, COUNT
OPEN(UNIT=10, FILE='c141jl18.dat', STATUS='OLD')
OPEN(UNIT=20, FILE='c141cl18.dat', STATUS='OLD')
OPEN(UNIT=30, FILE='c141l18.dat', STATUS='NEW')
DO 15  I = 1,150
  READ(10,*) COUNT,TT,TI, XJ, YJ, ZJ
  READ(20,*) COUNT,TT,TI, XC, YC, ZC
  XM = (XJ+XC)/2
  YM = (YJ+YC)/2
  ZM = (ZJ+ZC)/2
    XD = ABS(XJ - XC)
          DIST = XD
  IF (TI .GT.3.0 .AND. DIST .LT. 3.0) THEN
      STOP
   ELSE
 WRITE(30,*) I,TI,XM,YM,ZM
  END IF
   15 CONTINUE
STOP
END
```

Appendix B. Program 2

This Fortran program calculates minimum distances between each left and right jumper on the interval of +.5 to -.5 seconds (130 Knots = 219.4 feet/second).

```
cccccccccccccccccccccccccccccccccccccccccccccccccccccccccccccccccccccccc
VARIABLE DICTIONARY
C   LCNT = LEFT COUNT
C   RCNT = RIGHT COUNT
C   LCOUNT = LEFT COUNT
C   RCOUNT = RIGHT COUNT
C   LINDEX = LEFT INDEX
C   RINDEX = RIGHT INDEX
C   DIST = DISTANCE BETWEEN LEFT AND RIGHT JUMPER TRAJECTORY
C         MINDIST = MINIMUM DISTANCE
C   TIMEINT = TIME INTERVAL
cccccccccccccccccccccccccccccccccccccccccccccccccccccccccccccccccccccccc
C  DECLARE VARIABLE TYPES
INTEGER LCNT, RCNT
INTEGER LCOUNT(19), RCOUNT(20)
INTEGER LINDEX(101), RINDEX(101)
REAL  XD,YD,ZD,DIST
REAL  TL(101),TR(101),XL(101),XR(101),YL(101),YR(101)
        REAL  ZL(101),ZR(101),TIMEINT, MINDIST(21)
REAL  TMP_MINDIST
CHARACTER *11, LFN(19), RFN(20)
DATA LCOUNT /93,97,97,93,88,100,94,86,88,85,92,96,89,96,95,93,95,95,88/
DATA RCOUNT /100,101,90,90,88,89,91,94,92,92,79,93,97,87,84,88,83,94,96,96/
DATA LFN/'c141l01.dat','c141l02.dat','c141l03.dat','c141l04.dat'
     ,'c141l05.dat','c141l06.dat','c141l07.dat','c141l08.dat'
     ,'c141l09.dat','c141l10.dat','c141l11.dat','c141l12.dat'
     ,'c141l13.dat','c141l14.dat','c141l15.dat','c141l16.dat'
     ,'c141l17.dat','c141l18.dat','c141l19.dat'/
DATA RFN/'c141r01.dat','c141r02.dat','c141r03.dat','c141r04.dat'
     ,'c141r05.dat','c141r06.dat','c141r07.dat','c141r08.dat'
     ,'c141r09.dat','c141r10.dat','c141r11.dat','c141r12.dat'
     ,'c141r13.dat','c141r14.dat','c141r15.dat','c141r16.dat'
     ,'c141r17.dat','c141r18.dat','c141r19.dat','c141r20.dat'/
OPEN(UNIT=30, FILE='MINDISC141.DAT', STATUS='NEW')
DO 777 M=1,19
   OPEN(UNIT=10, FILE=LFN(M), STATUS='OLD')
       DO 35  I = 1, LCOUNT(M)
```

```
      READ(10,*) LINDEX(I), TL(I), XL(I), YL(I), ZL(I)
 35    CONTINUE
   DO 888 N=1,20
            OPEN(UNIT=20, FILE=RFN(N), STATUS='OLD')
    DO 45 J = 1, RCOUNT(N)
         READ(20,*) RINDEX(J), TR(J), XR(J), YR(J), ZR(J)
 45 CONTINUE
K = 1
  DO 50 TIMEINT = -0.5/0.05, 0.5/0.05, 0.05/0.05
     IF (TIMEINT .GT. 0.0) THEN
      DO 210 RCNT = 1,RCOUNT(N)
XR(RCNT) = XR(RCNT) + TIMEINT*219.4*0.05
 210       CONTINUE
   ELSE
      DO 220 LCNT = 1,LCOUNT(M)
XL(LCNT) = XL(LCNT) - TIMEINT*219.4*0.05
 220        CONTINUE
   ENDIF
   I = 1
   J = 1
   L = 1
   TMP_MINDIST = 9999.0
 70    IF (TIMEINT .GT. 0.0) THEN
      I = J + TIMEINT
   ELSE
      J = I - TIMEINT
   END IF
    XD = (XL(I) - XR(J))**2
    YD = (YL(I) - YR(J))**2
    ZD = (ZL(I) - ZR(J))**2
    DIST = SQRT(XD + YD + ZD)
    IF (TMP_MINDIST .GT. DIST) THEN
       TMP_MINDIST = DIST
    END IF
   L = L + 1
   I = I + 1
   J = J + 1
    IF (I .GT. LCOUNT(M) .OR. J .GT. RCOUNT(N) ) THEN
       MINDIST(K) =  TMP_MINDIST
       K = K + 1
IF (TIMEINT .GT. 0.0) THEN
         DO 230 RCNT = 1,RCOUNT(N)
```

```
      XR(RCNT) = XR(RCNT) - TIMEINT*219.4*0.05
 230           CONTINUE
       ELSE
          DO 240 LCNT = 1,LCOUNT(M)
      XL(LCNT) = XL(LCNT) + TIMEINT*219.4*0.05
 240            CONTINUE
       ENDIF
       GO TO 50
      ELSE
       GO TO 70
      END IF
 50 CONTINUE
DO 100 K = 1, 21
   WRITE(30,*)  MINDIST(K)
 100 CONTINUE
CLOSE(UNIT=20)
 888 CONTINUE
CLOSE(UNIT=10)
 777 CONTINUE
STOP
END
```

Appendix C. Program 3

This program computes minimum distance using the bootstrap method for 50%, 60%, 70%, 80%, 90%, and 95% confidence bounds from the set of original experimental data (130Knots = 219.4 feet/seond).

```
CCCCCCCCCCCCCCCCCCCCCCCCCCCCCCCCCCCCCCCCCCCCCCCCCCCCCCCCCCCCCCCCCCCCCCCC
VARIABLE DICTIONARY
C   ORIGC141 = ORIGINAL MINIMUM DISTANCE DATA SET
C         UNSRTC141 = UNSORTED EACH BOOTSTRAP MINIMUM DISTANCE DATA SET
C   TLIMIT = BOOTSTRAP ITERATIONS
CCCCCCCCCCCCCCCCCCCCCCCCCCCCCCCCCCCCCCCCCCCCCCCCCCCCCCCCCCCCCCCCCCCCCCCC
C  DECLARE VARIABLE TYPES
REAL ORIGC141(7980)
REAL UNSRTC141(7980,1000)
REAL     LB95(7980),MB95(7980),UB95(7980)
REAL     LB90(7980),UB90(7980),LB80(7980),UB80(7980)
REAL     LB70(7980),UB70(7980),LB60(7980),UB60(7980),LB50(7980),UB50(7980)
INTEGER CNT, LI(19), RI(20)
INTEGER LEFTOFF, RGTOFF
PARAMETER (N = 7980)
PARAMETER (M = 1000)
REAL RA(N), RB(N), RC(M), RD(M), TEMP(7980,1000)
EXTERNAL SVRGN
OPEN(UNIT=30, FILE='MINDISC141.DAT', STATUS='OLD')
OPEN(UNIT=50, FILE='left.1000.dat', STATUS='OLD')
OPEN(UNIT=60, FILE='right.1000.dat', STATUS='OLD')
OPEN(UNIT=40, FILE='SORT25.DAT', STATUS='NEW')
OPEN(UNIT=70, FILE='SORT500.DAT', STATUS='NEW')
OPEN(UNIT=90, FILE='SORT975.DAT', STATUS='NEW')
OPEN(UNIT=110, FILE='SORT50.DAT', STATUS='NEW')
OPEN(UNIT=120, FILE='SORT950.DAT', STATUS='NEW')
OPEN(UNIT=130, FILE='SORT100.DAT', STATUS='NEW')
OPEN(UNIT=140, FILE='SORT900.DAT', STATUS='NEW')
OPEN(UNIT=150, FILE='SORT150.DAT', STATUS='NEW')
OPEN(UNIT=160, FILE='SORT850.DAT', STATUS='NEW')
OPEN(UNIT=170, FILE='SORT200.DAT', STATUS='NEW')
OPEN(UNIT=180, FILE='SORT800.DAT', STATUS='NEW')
OPEN(UNIT=190, FILE='SORT250.DAT', STATUS='NEW')
OPEN(UNIT=200, FILE='SORT750.DAT', STATUS='NEW')
READ(30,*) (ORIGC141(LIMIT), LIMIT=1,7980)
C  GENERATE POSSIBLE MINIMUM DISTANCE OF 1000 BOOTSTRAP ITERATIONS AND
```

```
C  SORT EACH BOOTSTRAP ITERATION (COLUMN SORT)
DO 1000 TLIMIT = 1, 1000
CNT = 0
READ(50, *) (LI(I), I=1,19)
READ(60, *) (RI(I), I=1,20)
DO 600 I = 1,19
   LEFTOFF = (LI(I)-1)*20*21
   DO 700 J = 1, 20
RGTOFF  = (RI(J)-1)*21
DO 800 K = 1, 21
    CNT = CNT + 1
    UNSRTC141(CNT,TLIMIT) = ORIGC141(LEFTOFF + RGTOFF + K)
           RA(CNT) = UNSRTC141(CNT,TLIMIT)
800 CONTINUE
700    CONTINUE
600 CONTINUE
CALL SVRGN (N,RA,RB)
DO L = 1 ,7980
TEMP(L,TLIMIT) = RB(L)
END DO
1000 CONTINUE
C  SORT EACH ROWS AND GET 25, 50, 100, ... , 950, 975TH COLUMNS AS
C  95%, 90%, ..., 60%, AND 50% BOOTSTRAP CONFIDENCE INTERVALS
DO  TLIMIT = 1, 7980
  DO L = 1 ,1000
  RC(L) = TEMP(TLIMIT,L)
  END DO
  CALL SVRGN (M,RC,RD)
  DO L = 1 ,1000
  TEMP(TLIMIT,L) = RD(L)
  END DO
       END DO
DO 4000 K = 1, 7980
   LB95(K) = TEMP(K,25)
   MB95(K) = TEMP(K,500)
   UB95(K) = TEMP(K,975)
   LB90(K) = TEMP(K,50)
   UB90(K) = TEMP(K,950)
   LB80(K) = TEMP(K,100)
   UB80(K) = TEMP(K,900)
   LB70(K) = TEMP(K,150)
   UB70(K) = TEMP(K,850)
```

```
      LB60(K) = TEMP(K,200)
      UB60(K) = TEMP(K,800)
      LB50(K) = TEMP(K,250)
      UB50(K) = TEMP(K,750)
      WRITE(40,*) LB95(K)
      WRITE(70,*) MB95(K)
      WRITE(90,*) UB95(K)
      WRITE(110,*) LB90(K)
      WRITE(120,*) UB90(K)
      WRITE(130,*) LB80(K)
      WRITE(140,*) UB80(K)
      WRITE(150,*) LB70(K)
      WRITE(160,*) UB70(K)
      WRITE(170,*) LB60(K)
      WRITE(180,*) UB60(K)
      WRITE(190,*) LB50(K)
      WRITE(200,*) UB50(K)
4000 CONTINUE
STOP
END
```

Appendix D. Bootstrap Confidence Bounds Plots

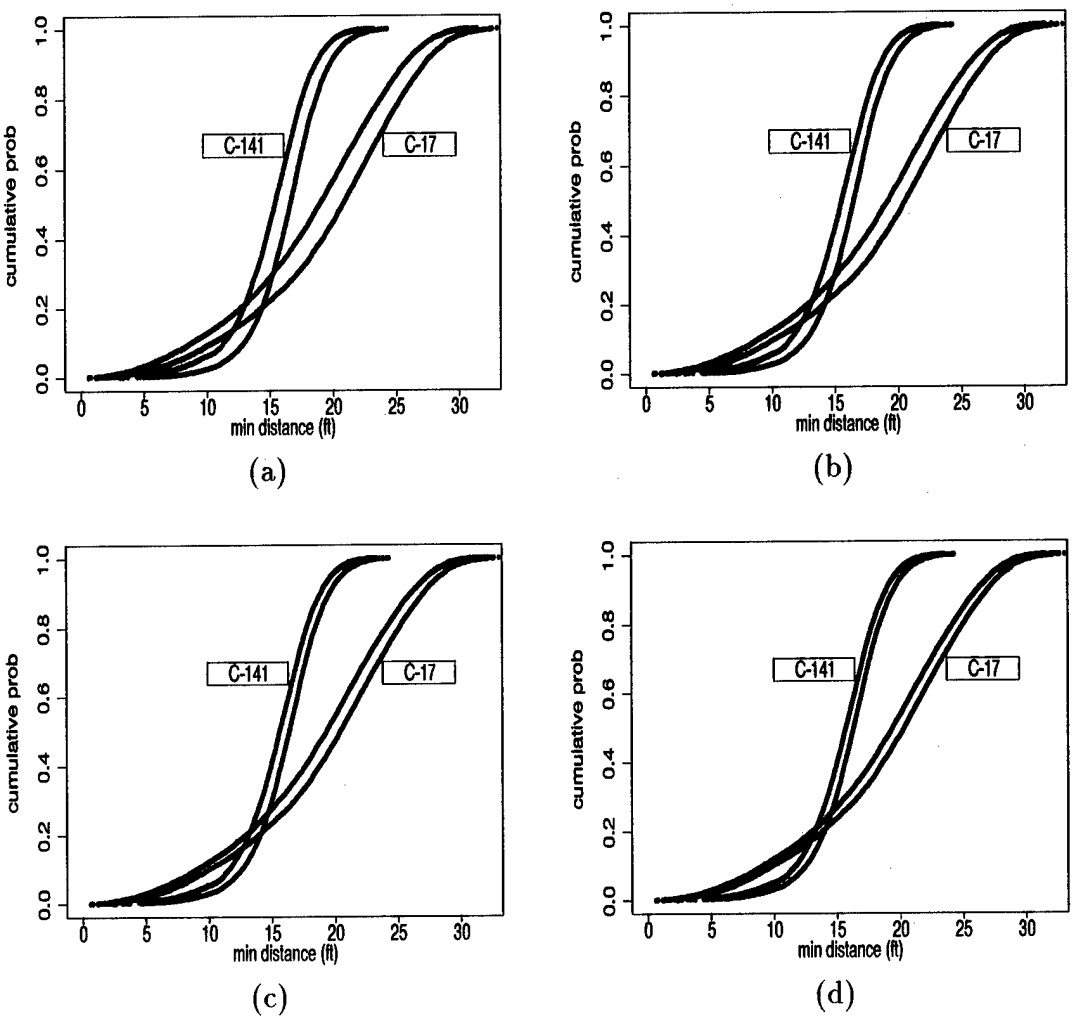

Figure D.1 Comparing Bootstrap Confidence bounds between C-141 vs. November C-17: (a) 90% bootstrap confidence bounds (b) 80% bootstrap confidence bounds, (c) 70% bootstrap confidence bounds, (d) 60% bootstrap confidence bounds.

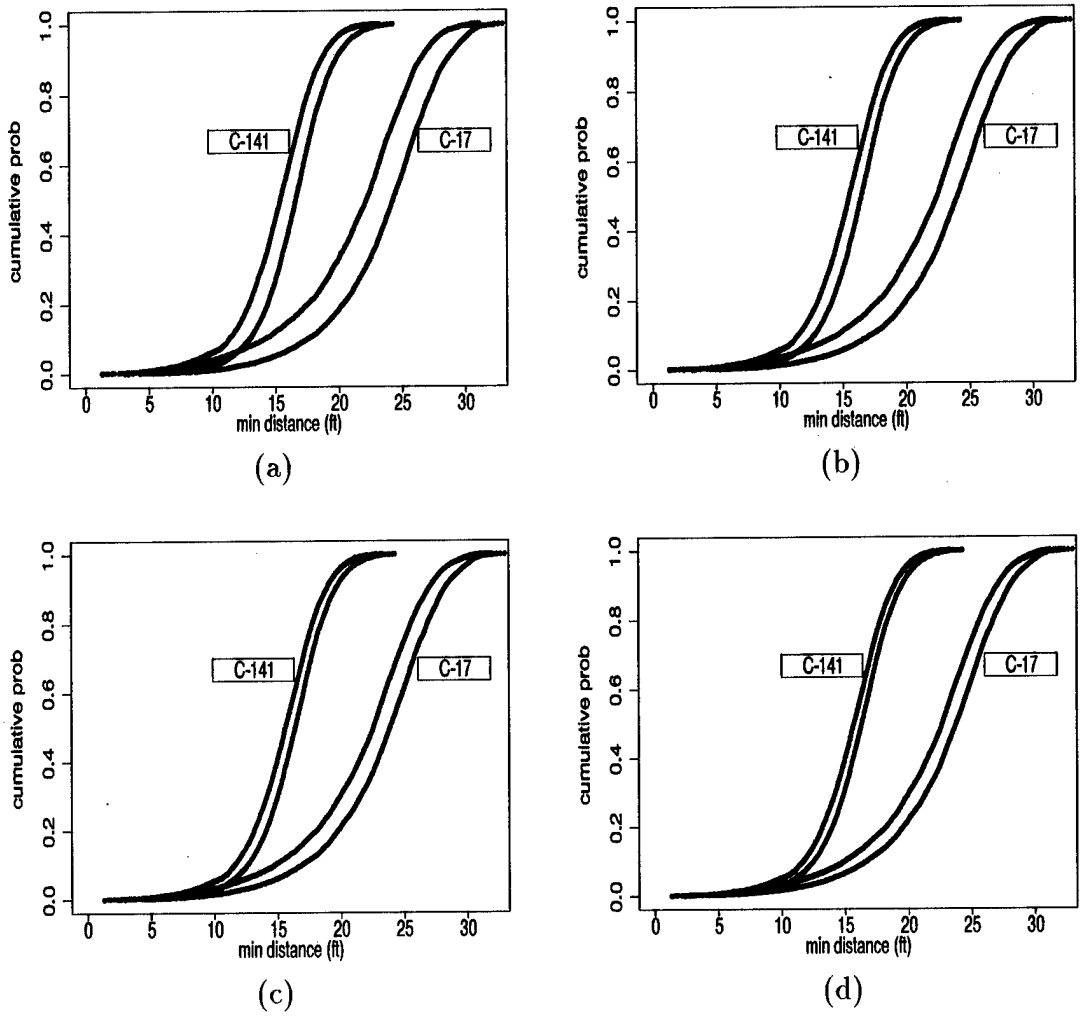

Figure D.2 Comparing Bootstrap Confidence bounds between C-141 vs. March C-17: (a) 90% bootstrap confidence bounds (b) 80% bootstrap confidence bounds, (c) 70% bootstrap confidence bounds, (d) 60% bootstrap confidence bounds.

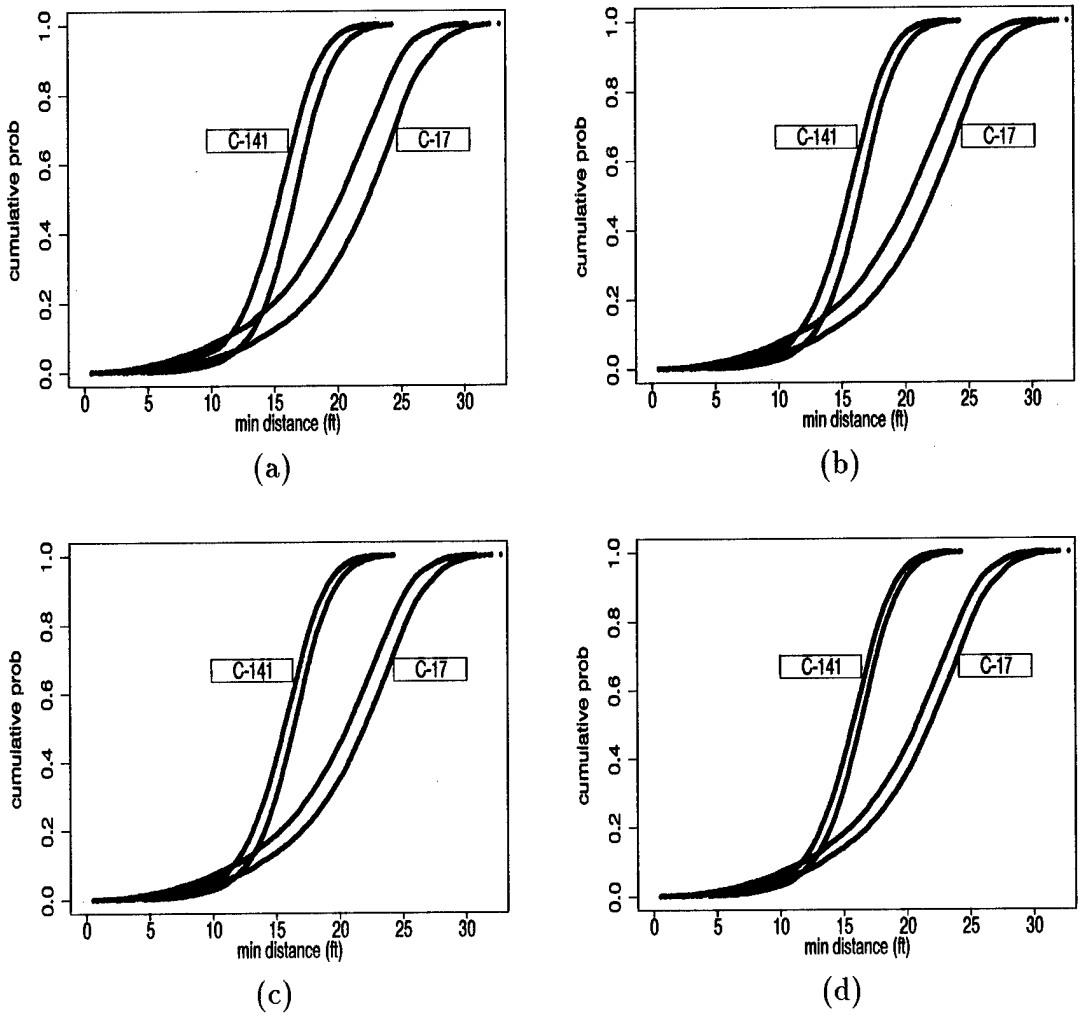

Figure D.3 Comparing Bootstrap Confidence bounds between C-141 vs. March heavy C-17: (a) 90% bootstrap confidence bounds (b) 80% bootstrap confidence bounds, (c) 70% bootstrap confidence bounds, (d) 60% bootstrap confidence bounds.

Bibliography

1. The Boeing Co. (1990). *CREST EASY5w Simulation User's Manual.*
2. Box, G.E.P., Hunter, W.G. and Hunter, J.S. (1978). *Statistics for Experimenters: An Introduction to Design, Data Analysis, and Model Building.* John Wiley & Sons.
3. Boos, D. and Monahan, J. (1986). "Bootstrap methods using prior information." *Biometrika* **73**, 77–83.
4. Byrne, D.M. and Taguchi, S. (1987). "The Taguchi Approach to Parameter Design." *Quality Progress*, **20**, 19–26, December.
5. Cox, D.R. (1973). "Regression Models and LifeTables." *J. R. Statist. Soc.* B **34**, 187–220.
6. DiCiccio, T.J. (1988). "A review of bootstrap confidence intervals (with discussion)." *J.Royal. Statist. Soc.* B **50**, 338–370.
7. Efron, B. and Tibshirani, R. J. (1993).*An Introduction to the Bootstrap.* Chapman & Hall, Inc.
8. Efron, B. (1979). "Bootstrap Methods: Another Look at the Jackknife." *Ann. Statist.* **7**, 1–26.
9. Efron, B. (1981). "Censored Data and the Bootstrap." *J. Amer. Statist. Assoc.* **76**, 312–319.
10. Gelfand, A. and Smith, A. F. M. (1990). "Sampling-based approaches to calculating marginal densities." *J. Amer. Statist. Assoc.* **85**, 398–409.
11. Kaplan, E.L. and Meier, P. (1958). "Non-parametric Estimation from Incomplete Observations." *J. Amer. Statist. Assoc.* **53**, 457–481.
12. Lawson, Kevin L. (1995). "Personnel Airdrop Optimization via Design of Experiments Methods" Department of Mathematics and Statistics School of Engineering Air Force Institute of Technology.
13. Lawson, Kevin L. (July 20, 1995). "Personnel Airdrop Optimization via Design of Experiments" Department of Mathematics and Statistics School of Engineering Air Force Institute of Technology.
14. Montgomery, D. C. (1991). *Design and Analysis of Experiments.* John Wiley & Sons.
15. Rogers, L. C. (1994). "Computational Analysis Method for Assessing the Collision Potential between Aircrew and Aircraft During Bailout." 32nd Annual SAFE Symposium Proceedings.
16. Mendenhall, W., Wackerly, D.D. and Scheaffer, R.L. (1990). *Mathematical Statistics with Applications.* Duxbury Press.

Vita

Major Won-sik Kim was born 14 March 1963 in Incheon, Republic of Korea, the son of Dal-yun and Eun-soon Kim. He graduated from the Daegun high school in 1981 and entered the Korea Military Academy from which he received the degree of Bachelor of Science in Electronic Engineering in March 1985. Upon graduation he was commissioned in the R.O.K. Army. He began active duty and served as a platoon leader and company commander in Air-Defense Artillery. He then served as an Instructor for the Department of Air-Defense at the Army Infantry School in Daegu until entering the Air Force Institute of Technology, School of Engineering,Wright-Patterson Air Force Base, Ohio, in June 1994.

Permanent address: 403-130
186-283 Shipjeong Dong Bupyung-Gu
Incheon, Republic of Korea

REPORT DOCUMENTATION PAGE

Form Approved
OMB No. 0704-0188

1. AGENCY USE ONLY (Leave blank)	2. REPORT DATE	3. REPORT TYPE AND DATES COVERED
	December 96	Master's Thesis

4. TITLE AND SUBTITLE
Personnel Airdrop Risk Assessment Using Bootstrap Sampling

5. FUNDING NUMBERS

6. AUTHOR(S)
Won Sik Kim, Major, ROKA

7. PERFORMING ORGANIZATION NAME(S) AND ADDRESS(ES)
Air Force Institute of Technology
WPAFB OH 45433-6583

8. PERFORMING ORGANIZATION REPORT NUMBER
AFIT/GOR/ENS/96D-01

9. SPONSORING/MONITORING AGENCY NAME(S) AND ADDRESS(ES)
Mr. Mark A. Kuntavanish
C-17 SPO
WPAFB OH 45433-6583

10. SPONSORING/MONITORING AGENCY REPORT NUMBER

11. SUPPLEMENTARY NOTES

12a. DISTRIBUTION/AVAILABILITY STATEMENT
Approved for Public release; Distribution Unlimited.

12b. DISTRIBUTION CODE

13. ABSTRACT *(Maximum 200 words)*

Previous work on personnel airdrop problems involving jumpers has been event-oriented - entanglement rates, number of canopy "bumps", landing injuries, and deaths represent the typical metrics. The thesis expands this area of research by developing cumulative distribution functions of maximum possible chute entanglement risk for the C-17 using bootstrap techniques. By comparing the effects of various C-17 aircraft configurations on the entanglement CDF, this thesis shows that under certain configurations the risk of centerline entanglement for the C-17 is less than for the C-141.

14. SUBJECT TERMS
Experimental Design; Bootstrap Sampling; Modeling.

15. NUMBER OF PAGES
84

16. PRICE CODE

17. SECURITY CLASSIFICATION OF REPORT	18. SECURITY CLASSIFICATION OF THIS PAGE	19. SECURITY CLASSIFICATION OF ABSTRACT	20. LIMITATION OF ABSTRACT
Unclassified	Unclassified	Unclassified	UL

GENERAL INSTRUCTIONS FOR COMPLETING SF 298

The Report Documentation Page (RDP) is used in announcing and cataloging reports. It is important that this information be consistent with the rest of the report, particularly the cover and title page. Instructions for filling in each block of the form follow. It is important to ***stay within the lines*** to meet ***optical scanning requirements***.

Block 1. Agency Use Only *(Leave blank)*.

Block 2. Report Date. Full publication date including day, month, and year, if available (e.g. 1 Jan 88). Must cite at least the year.

Block 3. Type of Report and Dates Covered. State whether report is interim, final, etc. If applicable, enter inclusive report dates (e.g. 10 Jun 87 - 30 Jun 88).

Block 4. Title and Subtitle. A title is taken from the part of the report that provides the most meaningful and complete information. When a report is prepared in more than one volume, repeat the primary title, add volume number, and include subtitle for the specific volume. On classified documents enter the title classification in parentheses.

Block 5. Funding Numbers. To include contract and grant numbers; may include program element number(s), project number(s), task number(s), and work unit number(s). Use the following labels:

C	- Contract	**PR**	- Project
G	- Grant	**TA**	- Task
PE	- Program Element	**WU**	- Work Unit Accession No.

Block 6. Author(s). Name(s) of person(s) responsible for writing the report, performing the research, or credited with the content of the report. If editor or compiler, this should follow the name(s).

Block 7. Performing Organization Name(s) and Address(es). Self-explanatory.

Block 8. Performing Organization Report Number. Enter the unique alphanumeric report number(s) assigned by the organization performing the report.

Block 9. Sponsoring/Monitoring Agency Name(s) and Address(es). Self-explanatory.

Block 10. Sponsoring/Monitoring Agency Report Number. *(If known)*

Block 11. Supplementary Notes. Enter information not included elsewhere such as: Prepared in cooperation with...; Trans. of...; To be published in.... When a report is revised, include a statement whether the new report supersedes or supplements the older report.

Block 12a. Distribution/Availability Statement. Denotes public availability or limitations. Cite any availability to the public. Enter additional limitations or special markings in all capitals (e.g. NOFORN, REL, ITAR).

- **DOD** - See DoDD 5230.24, "Distribution Statements on Technical Documents."
- **DOE** - See authorities.
- **NASA** - See Handbook NHB 2200.2.
- **NTIS** - Leave blank.

Block 12b. Distribution Code.

- **DOD** - Leave blank.
- **DOE** - Enter DOE distribution categories from the Standard Distribution for Unclassified Scientific and Technical Reports.
- **NASA** - Leave blank.
- **NTIS** - Leave blank.

Block 13. Abstract. Include a brief *(Maximum 200 words)* factual summary of the most significant information contained in the report.

Block 14. Subject Terms. Keywords or phrases identifying major subjects in the report.

Block 15. Number of Pages. Enter the total number of pages.

Block 16. Price Code. Enter appropriate price code *(NTIS only)*.

Blocks 17. - 19. Security Classifications. Self-explanatory. Enter U.S. Security Classification in accordance with U.S. Security Regulations (i.e., UNCLASSIFIED). If form contains classified information, stamp classification on the top and bottom of the page.

Block 20. Limitation of Abstract. This block must be completed to assign a limitation to the abstract. Enter either UL (unlimited) or SAR (same as report). An entry in this block is necessary if the abstract is to be limited. If blank, the abstract is assumed to be unlimited.